

ARTEMIS Mission Design

Theodore H. Sweetser · Stephen B. Broschart · Vassilis Angelopoulos ·
Gregory J. Whiffen · David C. Folta · Min-Kun Chung · Sara J. Hatch ·
Mark A. Woodard

Received: 19 May 2011 / Accepted: 17 February 2012 / Published online: 24 March 2012
© Springer Science+Business Media B.V. 2012

Abstract The ARTEMIS mission takes two of the five THEMIS spacecraft beyond their prime mission objectives and reuses them to study the Moon and the lunar space environment. Although the spacecraft and fuel resources were tailored to space observations from Earth orbit, sufficient fuel margins, spacecraft capability, and operational flexibility were present that with a circuitous, ballistic, constrained-thrust trajectory, new scientific information could be gleaned from the instruments near the Moon and in lunar orbit. We discuss the challenges of ARTEMIS trajectory design and describe its current implementation to address both heliophysics and planetary science objectives. In particular, we explain the challenges imposed by the constraints of the orbiting hardware and describe the trajectory solutions found in prolonged ballistic flight paths that include multiple lunar approaches, lunar flybys, low-energy trajectory segments, lunar Lissajous orbits, and low-lunar-periapse orbits. We conclude with a discussion of the risks that we took to enable the development and implementation of ARTEMIS.

Keywords ARTEMIS · THEMIS · Low-energy transfer · Lissajous orbits · Lunar science · Lunar mission · Heliophysics · Magnetosphere

1 Introduction

Time History of Events and Macroscale Interactions during Substorms (THEMIS) is a very successful NASA Explorer mission launched in February of 2007 to advance our understanding of magnetic substorms, a space weather phenomenon in the Earth's magnetosphere (Angelopoulos 2008). The mission consists of five identical Earth-orbiting spacecraft

T.H. Sweetser (✉) · S.B. Broschart · V. Angelopoulos · G.J. Whiffen · M.-K. Chung · S.J. Hatch
Jet Propulsion Laboratory, California Institute of Technology, 4800 Oak Grove Dr., M/S, 301-121,
Pasadena, CA 91109, USA
e-mail: Ted.Sweetser@jpl.nasa.gov

D.C. Folta · M.A. Woodard
Goddard Space Flight Center, Greenbelt, MD, USA

(probes) equipped with particle and field instruments (Harvey et al. 2008). As of the time of this writing, the baseline mission science objectives have been achieved, and all five probes (and their instruments) are fully functional.

In February 2008 ARTEMIS, the Acceleration, Reconnection, Turbulence and Electrodynamics of the Moon's Interaction with the Sun mission, was proposed to the NASA Heliophysics Senior Review (Angelopoulos and Sibeck 2008) as an extension to the THEMIS mission. It was approved for development in May of that year. The ARTEMIS mission proposed to send the two outermost THEMIS probes, P1 and P2 (also referred to as THEMIS-B and THEMIS-C), to lunar orbits by way of two circuitous transfers that take about one and a half years each. The goals of the mission as proposed in 2008 were to use the Moon as an anchor for the ARTEMIS probes to conduct studies of Earth's magnetotail and solar wind from approximately 60 Earth radii and to study the lunar wake and its refilling as a function of the upstream solar wind. ARTEMIS two-point measurements open a new vantage point to phenomena previously studied by single-spacecraft missions. In particular, when solar wind measurements are made simultaneously by one probe in the lunar wake and the second from various locations just upstream of the lunar wake, accurate comparisons of wake phenomena with upstream variations can be made.

The ARTEMIS proposal represented the combined efforts of the THEMIS science team led by the PI at UCLA, the THEMIS Mission Operations team led by the Mission Operations Manager at the University of California Berkeley's Space Science Laboratory (UCB-SSL), the NASA Goddard Space Flight Center (GSFC), and the Jet Propulsion Laboratory at the California Institute of Technology (JPL). Two earlier reports (Broschart et al. 2009; Woodard et al. 2009) describe the preliminary mission design as proposed in 2008; portions of this paper are taken from those reports. This paper presents the evolution of the trajectory design to the trajectory being flown today, only a few months after lunar orbit delivery.

Numerous challenges were inherent to the ARTEMIS mission's trajectory design because of the constrained capabilities of the THEMIS probes. Limited fuel remained after the THEMIS baseline mission was completed. Thruster configuration limits thrust directions to one hemisphere. Additionally, an on-off thruster duty cycle imposed due to the spinning of the probe bus restricts effective thrust to less than a newton in the spin plane, i.e., for maneuver directions near the ecliptic plane. Maneuvers cannot be done in shadow because accurate pulse timing relies on sun-sensor data. Telecommunications with the probes were limited to a range of about two million kilometers. Finally, the probes can only withstand up to a 4-hour shadow. Had nothing been done at the end of the THEMIS baseline mission, long eclipses (> 8 hr) would have neutralized P1 by March 2010 (Angelopoulos 2010). This became a very significant driver for proposing the ARTEMIS mission.

In Sect. 2 we describe the capabilities and orbit configuration of the THEMIS probes at the end of their baseline mission. In Sect. 3 we outline the history of the ARTEMIS mission design concept as it followed the mission's programmatic evolution. Section 4 outlines the science goals and orbit design goals of the mission. The remainder of the paper describes the design of the trajectories that have taken P1 and P2 from eccentric, high-altitude Earth orbits into lunar orbits that satisfy the science objectives. Figure 1 shows the ARTEMIS trajectory design used to send P1 and P2 from their respective Earth orbits at the start of ARTEMIS maneuvers into lunar Lissajous orbits. Section 5 presents the most up-to-date ARTEMIS mission design. Section 6 describes the current mission status, including ongoing trade studies. Section 7 is a retrospective on the challenges and enabling attributes of the mission design effort.

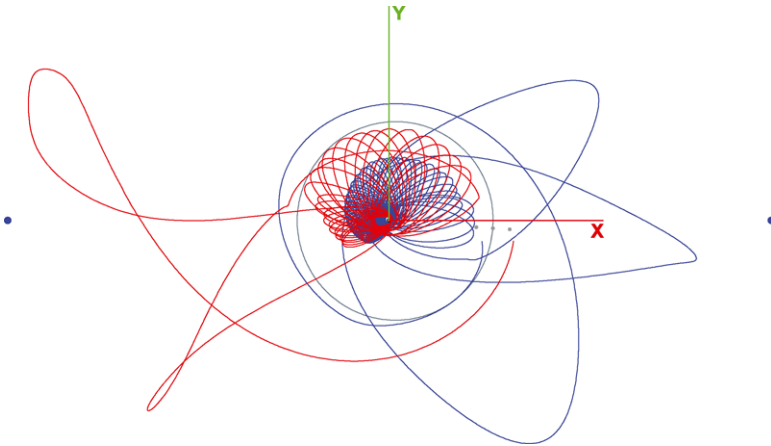
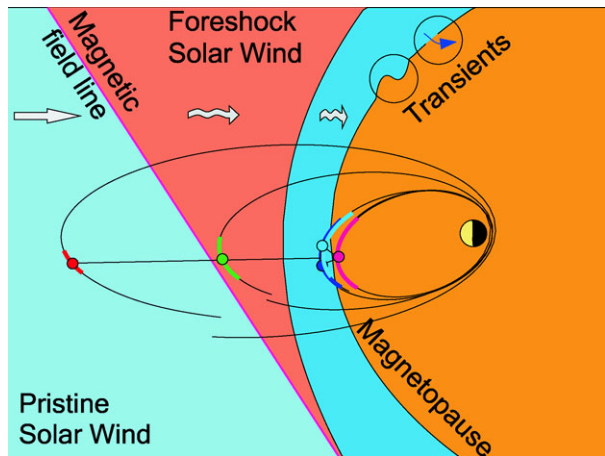


Fig. 1 ARTEMIS trans-lunar trajectories in the ecliptic plane. The coordinate frame here rotates such that the Sun is always to the left. The *red line* shows the P1 trajectory; the *blue line* shows the P2 trajectory. The Earth is at the center of the figure, and the Moon's orbit is shown in gray. The *blue dots* are the Sun-Earth L1 and L2 Lagrange points; the *gray dots* are the Moon and the Earth-Moon L1 and L2 points at a particular epoch

Fig. 2 THEMIS mission orbit configuration. *Filled circles* represent THEMIS probe locations during a dayside conjunction (*red*: P1 4-day orbit, *green*: P2 2-day orbit, *black*: P3 1-day orbit, *blue*: P4 1-day orbit, *pink*: P5 1-day orbit). The orbit geometries are indicated by *black lines*



2 Spacecraft Overview

On February 17th, 2007, the five THEMIS probes were launched on a Delta-II 7925 rocket into a 1.3-day Earth orbit with perigee at 437 km altitude and apogee at ~ 87500 km altitude (Angelopoulos 2008). Based on initial on-orbit data—in particular, better link margin performance—THEMIS-B was assigned to a 4-day orbit and designated “P1”, and THEMIS-C was assigned to a 2-day orbit and designated “P2”. THEMIS-D, E, and A were assigned to 1-day orbits, becoming P3, 4 and 5, respectively, per the mission design plan (Frey et al. 2008) required to achieve THEMIS mission science goals (Fig. 2) (Angelopoulos 2008). After 29 months in orbit, the two outermost probes, P1 and P2, were called on to journey to the Moon as part of the ARTEMIS mission.

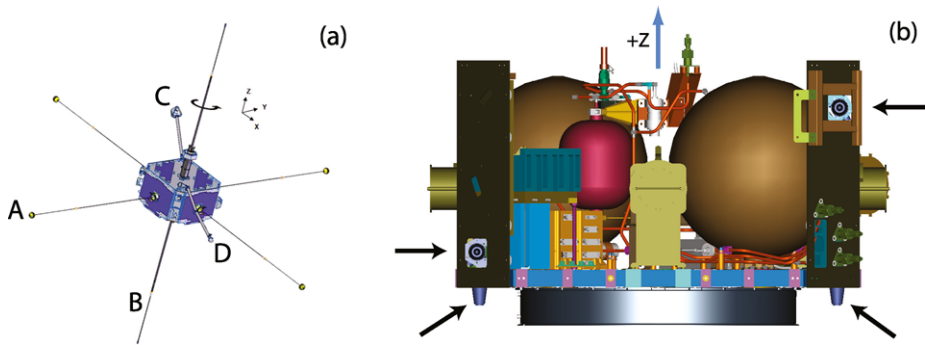


Fig. 3 THEMIS/ARTEMIS probe configuration. The probe buses were manufactured by ATK Space Systems (formerly Swales Aerospace), and the instruments were manufactured under the leadership of the University of California, Berkeley with both US and international collaborators. (a) On-orbit configuration with booms deployed, adapted from Auslander et al. (2008): A—four 20 m long radial EFI booms; B—two 5 m long axial EFI booms; C—1 m long SCM boom; D—2 m long FGM boom (http://www.nasa.gov/images/content/164405main_THEMIS-Spacecraft_bus2.jpg), (b) probe bus schematic. Black arrows indicate locations of the 4.4 N hydrazine thrusters. Blue arrow indicates spin axis

The five THEMIS probes were identical at launch with 134 kg mass (including 49 kg of hydrazine monopropellant). Each measures approximately $0.8 \times 0.8 \times 1.0$ meters (Harvey et al. 2008). On orbit, each has deployed a number of instrument booms and is spin-stabilized at ~ 20 RPM. Figure 3(a) shows a THEMIS probe with booms deployed. Figure 3(b) shows a schematic of the bus design. The blue arrow, which indicates the spin vector, shall be referred to as the probe +Z direction.

Each probe has four thrusters, nominally 4.4 N each, with locations indicated by the black arrows in Fig. 3(b). Two provide axial thrust (acceleration in +Z direction) for large ΔV maneuvers and attitude control. The other two provide tangential thrust in the spin plane for small ΔV maneuvers and spin rate control. Note that the probes cannot apply acceleration in the $-Z$ direction. During the nominal THEMIS mission, P1 and P2 were flown with the $-Z$ axis close to the ecliptic north pole, i.e., in an “upside-down” configuration relative to ecliptic north and opposite the inner three probes. This was done to aid the main orbit correction maneuvers in the second year of THEMIS, which were designed to counteract lunar perturbations on the orbit plane (Frey et al. 2008). ARTEMIS would maintain the same orientation, as it is quite fuel-intensive to impart spin-axis changes to the probes. Thus, maneuvers towards ecliptic north could not be included in the ARTEMIS trajectory design. At launch, each probe had 960 m/s total ΔV capability (Harvey et al. 2008). At the start of ARTEMIS maneuvers the remaining ΔV (approximately 320 m/s for P1 and 467 m/s for P2) were available for the ARTEMIS trajectory design. Due to fuel tank depressurization (Sholl et al. 2007; Frey et al. 2008), each thruster is expected to produce between 2.4 N and 1.6 N force during the ARTEMIS mission.

Because the spacecraft is spinning the effective thrust of a sideways burn is further reduced, so a maneuver in a particular direction in the spin plane is performed by pulsing the thrusters on and off during each revolution. With a 60 deg pulse duration, the thrusters are on only one-sixth of the time (16.7% duty cycle). Because thrusters are swinging through an arc, the thrust in the desired direction is further reduced to 95.5% effective thrust; with a 40 deg duty cycle the thrusters average only one-ninth thrust, but lose only 2% in efficiency averaged through the arc of each pulse. Only the second reduction in each case influences

the effective I_{sp} , so a 40 deg duty cycle would be preferred to a 60 deg one except that lower thrust means longer burns during periapse passages, which would increase gravity losses.

The thermal and power systems have been designed to withstand shadowing from the Sun for up to three hours (Harvey et al. 2008). It was demonstrated in March of 2009, however, that a 4-hour shadow is survivable with appropriate precautions. This limit is therefore being used as the maximum allowable shadow duration for the ARTEMIS mission design, where “shadow” is defined to be less than 50% sunlight.

3 ARTEMIS Concept Development

The baseline THEMIS mission design included the expectation that P1 would experience inordinately long (>8 hr) shadows by March 2010. Although the apoapse altitude of the P1 orbit could have been reduced to prevent this, THEMIS scientists and JPL mission designers came up with the idea of sending P1 “up” instead of “down” in 2005. With THEMIS instrumentation, compelling science could be conducted near or at the Moon with a single probe. According to initial trajectory studies, a direct transfer from P1 Earth orbit to a 1500 km altitude by 18,000 km radius polar orbit at the Moon would require ~ 500 m/s of ΔV (not including margin or losses associated with long thrust arcs). This was well beyond P1’s expected ΔV capability at the end of the baseline mission. However, the remaining fuel appeared sufficient to transfer P1 from its Earth orbit to the desired eccentric lunar orbit by way of a lunar swing-by and low-energy transfer (Chung et al. 2005). When initiated by a lunar swing-by, this type of transfer does not require any less ΔV to leave Earth, but saves essentially all the ΔV cost of getting into a Lissajous orbit around one of the Earth-Moon Lagrange points. It does this by using solar gravity tidal perturbations to make the three-body energy change on the trajectory that would otherwise have to be done propulsively at arrival near the Moon. The fuel reserves on P2 offered similar capability, suggesting the possibility of sending two THEMIS probes to the Moon.

With the encouraging initial trajectory design results in hand, proposals for funding to support a detailed design study of low-energy trans-lunar trajectories, feasibility studies related to the THEMIS hardware, and optimization of the remaining THEMIS mission for P1 and P2 were made in 2006 and 2007. Although these proposals were not selected for funding, the science team continued concept development as time permitted.

In the summer of 2007, internal JPL funding became available to support an Explorer program Mission of Opportunity proposal for a THEMIS mission extension that would become ARTEMIS. A team from the JPL Inner Planets Mission Analysis group was convened to design trajectories to the Moon for P1 and P2. Building on the work done in 2005, the JPL team (working closely with the THEMIS science and mission operations teams) developed a workable trajectory within THEMIS probe constraints that provided the opportunity for a highly rewarding scientific mission. This formed the baseline trajectory of the current ARTEMIS mission. Midway through this preliminary design effort, NASA headquarters advised the ARTEMIS team that the new mission would be more appropriately proposed as an extended mission for THEMIS, rather than as a mission of opportunity. At around the same time, the mission operations team at UCB-SSL was augmented by navigators and maneuver designers at GSFC who contributed operations experience with Lissajous and translunar orbits to the design effort.

The complete preliminary design for the extended mission was presented to the Senior Review Board for the Heliophysics Division in February 2008 (Angelopoulos and Sibeck 2008); approval to proceed with detailed design was given in May of that year. The preliminary trajectory design that was presented to the Senior Review Board is described in

Broschart et al. (2009). This paper is an update of that earlier design paper; the design described there has changed significantly since the approval to proceed. As was understood at the time, the series of Earth orbits leading up to the initial lunar flybys needed to be significantly redesigned. More recently, a number of changes have been made in the science operations phase of ARTEMIS.

In 2009 it was recognized that significant additional scientific benefits from ARTEMIS could be obtained for the Planetary Division of NASA's Science Mission Directorate. The team was invited to propose an amendment to its Heliophysics plan that addressed Planetary objectives. The proposal was returned by NASA/HQ, and the invitation was re-extended for submission in the 2010 Senior Review cycle, so both Heliophysics and Planetary aspects of the ARTEMIS proposal could be evaluated by a joint panel. ARTEMIS/Heliophysics was given the go-ahead to continue operations in June 2010. The ARTEMIS/Planetary decision, though delayed until December 2010, was also positive. The 2008 preliminary design of ARTEMIS's lunar orbits needed to be modified to accommodate planetary objectives by lowering periape altitudes, raising inclinations, and adjusting the lines of apsides for better overlap of measurements with those of NASA's Lunar Atmosphere and Dust Environment Explorer (LADEE) mission.

The Planetary Division's decision to execute the planetary objectives of the mission came only 3 months prior to the baseline ARTEMIS lunar orbit insertion (originally slated for April 2011). This did not leave sufficient time for performing the necessary lunar orbit optimization to meet the expanded science objectives. Therefore, the team decided to postpone insertion to June-July 2011 to enable further study of the planetary aspects of the investigation. This postponement in turn entailed modifications to both the Lissajous phase and the transition to lunar orbits.

The ARTEMIS science objectives and the characteristics of orbits that would satisfy them (for both Heliophysics and Planetary Divisions of the Science Mission Directorate) as proposed and accepted by the 2010 Senior Review were described in Angelopoulos (2010). The revised mission design described in this paper represents the ARTEMIS orbit execution plan as actually implemented.

4 ARTEMIS Science Goals

Angelopoulos (2010) gives a comprehensive overview of ARTEMIS mission science objectives and describes how the mission design and operations are structured to meet them. Here we describe aspects of the mission that drive mission design.

Each probe is equipped with a suite of five particle and field instruments used to study geomagnetic substorm activity during the nominal THEMIS mission. These instruments include a Fluxgate Magnetometer, a Search Coil Magnetometer, an Electric Field Instrument, an Electrostatic Analyzer, and a Solid State Telescope (Angelopoulos 2008). This instrumentation suite allows the probe to measure the 3D distribution of thermal and super-thermal ions and electrons and the AC and DC magnetic and electric fields to study the interaction between the Earth's magnetic field and the Sun's magnetic field and solar wind. By expanding the spatial extent of THEMIS's multiple, identically-instrumented spacecraft, ARTEMIS allows us to study plasmoids in the magnetotail, particle acceleration and turbulence in the magnetotail and the solar wind. Furthermore, ARTEMIS will study lunar wake formation and evolution for the first time with two identical, nearby probes, thereby resolving spatio-temporal ambiguities. The aforementioned heliophysics objectives of the mission can be addressed by inter-spacecraft separations and wake downstream crossings that are

initially as large as 20 Earth radii and are progressively reduced to 1000 km or less. This goal is achieved initially by having the ARTEMIS probes at large separations in Lissajous orbits around two (and later one) of the Earth-Moon Lagrange points, and subsequently by insertion of probes into lunar orbits with $\sim 18,000$ km apoapse radius and highly variable angular separation between their lines of apsides.

ARTEMIS also offers a unique opportunity to contribute to planetary science. From its unique orbits ARTEMIS will study the “sources and transport of exospheric and sputtered species; charging and circulation of dust by electric fields; structure and composition of the lunar interior by electromagnetic (EM) sounding; and surface properties and planetary history, as evidenced in crustal magnetism. Additionally, ARTEMIS’s goals and instrumentation complement LRO’s [*Lunar Reconnaissance Orbiter’s*] extended phase measurements of the lunar exosphere and of the lunar radiation environment by providing high fidelity local solar wind data. ARTEMIS’s electric field and plasma data also support LADEE’s prime goal of understanding exospheric neutral particle and dust particle generation and transport” (Angelopoulos 2010).

To achieve these objectives, ARTEMIS requires both high- and low-altitude measurements by one spacecraft, while the other measures the pristine solar wind nearby. Low periapses are very important in increasing the ability of ARTEMIS to measure sputtered ions and crustal magnetism in situ. For this reason periapse altitudes less than 50 km are highly desired. Additionally, the latitude of periapsis is an important consideration for lunar crustal magnetism—increased periapsis latitude provides opportunities for covering a larger portion of the lunar surface. A latitude greater than 10 deg (goal 20 deg) is highly desirable. Finally, conjunctions with LADEE at the dawn terminator necessitate that one of the ARTEMIS probes have its periapsis positioned near the dawn terminator and pass through periapse close to the time of LADEE passage through that region. These design considerations have been incorporated into the current planning for the upcoming lunar orbit insertions (LOIs).

5 ARTEMIS Trajectory Design

Figure 1 shows the ARTEMIS trajectory design that sent P1 and P2 from their respective orbits at the end of the THEMIS primary mission to insertion into lunar Lissajous orbit. The P1 trajectory is shown in red, and the P2 trajectory is shown in blue. The design succeeded in meeting both the trajectory constraints imposed by the probe capabilities and the requirements derived from the science objectives.

In the following subsections, the trajectory is broken up into phases for detailed discussion. These include the Earth orbit phase, the trans-lunar phase, the Lissajous orbit phase, and the lunar orbit phase. An integrated timeline of the events for P1 and P2 in these four mission phases can be found in Table 1; an integrated ΔV budget is given in Table 2.

5.1 Earth Orbit Phase Trajectories

When the preliminary design was being developed to show the feasibility of ARTEMIS, the orbit raise did not appear to present any particular challenge, so this phase was simplified to a single impulsive velocity increase at perigee, followed by a number of Earth orbits including lunar approaches that modified the orbit and culminated in the lunar flyby that begins the low-energy transfer to the Moon. This simplification allowed one track of the design effort to focus most strongly on the lunar flyby and transfer; the series of finite orbit raise maneuvers (ORMs) to raise the Earth orbit could be developed later in parallel on a separate design track.

Table 1 Integrated trajectory design timeline

Earth-Orbit Phase	Jul 20, 2009	ARTEMIS mission begins
Earth-Orbit Phase	Jul 21, 2009	First P2 Orbit-Raise Maneuver
Earth-Orbit Phase	Aug 1, 2009	First P1 Orbit-Raise Maneuver
Earth-Orbit Phase	Oct 12, 2009	P1 Fly-by Targeting Maneuver 1
Earth-Orbit Phase	Dec 2, 2009	P1 Fly-by Targeting Maneuver 2
Earth-Orbit Phase/ Trans-Lunar Phase	Jan 31, 2010	P1 Lunar Fly-by #1 (min Range = 12600 km)
Trans-Lunar Phase	Feb 13, 2010	P1 Lunar Fly-by #2 (min Range = 3290 km)
Trans-Lunar Phase	Mar 10, 2010	P1 Deep-space Maneuver (+ Local Maximum Range = 1200000 km to Earth)
Earth-Orbit Phase	Mar 24, 2010	P2 Fly-by Targeting Maneuver
Earth-Orbit Phase/ Trans-Lunar Phase	Mar 28, 2010	P2 Lunar Fly-by (min Range = 8070 km)
Trans-Lunar Phase	Apr 13, 2010	P1 Earth Fly-by (min Range = 17000 km)
Trans-Lunar Phase	May 11, 2010	P2 Earth Fly-by #1 (min Range = 86000 km)
Trans-Lunar Phase	Jun 1, 2010	P2 Deep-space Maneuver 2
Trans-Lunar Phase	Jun 06, 2010	P1 Maximum Range (1,500,000 km to Earth)
Trans-Lunar Phase	Jun 18, 2010	P2 Maximum Range (1,200,000 km to Earth)
Trans-Lunar Phase	Jul 27, 2010	P2 Earth Fly-by #2 (min Range = 170000 km)
Trans-Lunar Phase/ Lissajous Orbit Phase	Aug 25, 2010	P1 LL2 Insertion
Trans-Lunar Phase/ Lissajous Orbit Phase	Oct 20, 2010	P2 LL1 Insertion
Lissajous Orbit Phase	Jan 01, 2011	P1 Departs LL2
Lissajous Orbit Phase	Jan 11, 2011	P1 LL1 Insertion
Lissajous Orbit Phase	Jun 18, 2011	P1 Lunar Transfer Initiation
Lissajous Orbit Phase	Jun 21, 2011	P2 Lunar Transfer Initiation 1
Lunar Orbit Phase	Jun 27, 2011	P1 LOI (1850 km alt)
Lissajous Orbit Phase	Jun 28, 2011	P2 Lunar Transfer Initiation 2
Lunar Orbit Phase	Jul 17, 2011	P2 LOI (3800 km alt)
Lunar Orbit Phase	Dec 28, 2012	P1 End of 1.5 year Lunar Orbit Phase
Lunar Orbit Phase	Jan 17, 2013	P2 End of 1.5 year Lunar Orbit Phase
LADEE Science Phase	Jul 7, 2013	Beginning, for earliest LADEE launch
LADEE Science Phase	Oct 15, 2013	End, for earliest LADEE launch
LADEE Science Phase	Dec 16, 2013	Beginning, for latest LADEE launch
LADEE Science Phase	Mar 26, 2014	End, for latest LADEE launch

Figure 4 shows the ARTEMIS P1 trajectory from the end of the nominal THEMIS mission through the first close lunar flyby. In the figure, the red line represents the ARTEMIS P1 trajectory starting with its orbit at the end of the THEMIS primary mission, and the gray circle indicates the Moon's orbit. The plot is centered on the Earth and shown in the Sun-Earth synodic coordinate frame, which rotates such that the Sun is fixed along the negative X axis (to the left) and the Z axis is aligned with the angular momentum of the Earth's heliocentric orbit. As time passes, the line of apsides of P1's geocentric orbit rotates clockwise in the main figure. The insert in the bottom left shows P1's motion out of the ecliptic plane, where

Table 2 ARTEMIS ΔV budget as proposed and actual (with italic values showing current estimates of lunar deorbit ΔV)

	P1 cost est. (m/s)	P1 cost act. (m/s)	P2 cost est. (m/s)	P2 cost act. (m/s)
ORMs	96.7	95.8	204.0	231.4
SDMs				11.0
FTMs	7.0	6.9	5.7	12.4
DSMs	4.8	7.3	15.1	30.2
LTI	1.5	3.2	0.8	1.0
LOIs	89.9	50.3	117.1	73.0
Lunar orbit periapee lowering		40.7		45.3
Deterministic DV total	200	204	343	404
Sources of additional DV cost:				
TLI declination penalty	(Included)	(Included)	(Included)	(Included)
TLI grav and steering loss (w/shadow)	(Included)	(Included)	36	(Included)
LOI declination penalty	2	(Included)	2	(Included)
LOI grav and steering loss	(Included)	(Included)	(Included)	(Included)
Lissajous maintenance	15	8.7	12	4.5
TCMs (3% + 1 m/s per ORM $\times \sqrt{(n)}$)	15	7.5	14	4.2
Total	232	221	407	413
Available DV	324	320	475	467
Margin	92	99	68	54
Liens against margin:				
Matching ORM phase to transfer phase	None		5	
Precession correction in ORM phase	1		2	
Lissajous maintenance increase	20		13	
End-of-mission deorbit	10	2	64	2

the largest plane change was caused by a lunar approach in December 2009. The labels on the plot provide information about key events during this phase of the mission.

The design of the P2 Earth orbits phase was similar, as shown in Fig. 5, but lasted two months longer because it started from a smaller Earth orbit and a longer series of finite maneuvers needed to be included to raise the orbit.

As we gradually came to realize, the reference trajectory design for the Earth orbit phase of both P1 and P2 would turn out to be significantly more complex than a simple series of maneuvers to replace the preliminary design's impulsive orbit raise maneuver. This complexity stemmed from: (1) probe operational constraints, (2) the tight ΔV budget, (3) the precision phasing required to reach the designed low-energy transfers to the Moon, and (4) the actual initial states for ARTEMIS P1, P2 in the summer of 2009. These actual states ended up significantly different from the initial states that were predicted in 2005–2007; this change was due to deterministic orbit-change maneuvers that occurred in 2008, mid-way through the THEMIS mission, to improve science yield for the second THEMIS tail season (Fig. 6 shows this difference for the P1 orbit). As expected, the actual orbit raise required perigee burns on multiple orbits due to the small thrust capability. The design of these burns was challenging because generally an optimal design of highly elliptical transfers is numerically difficult, and because lunar approaches created a complex three-body design space.

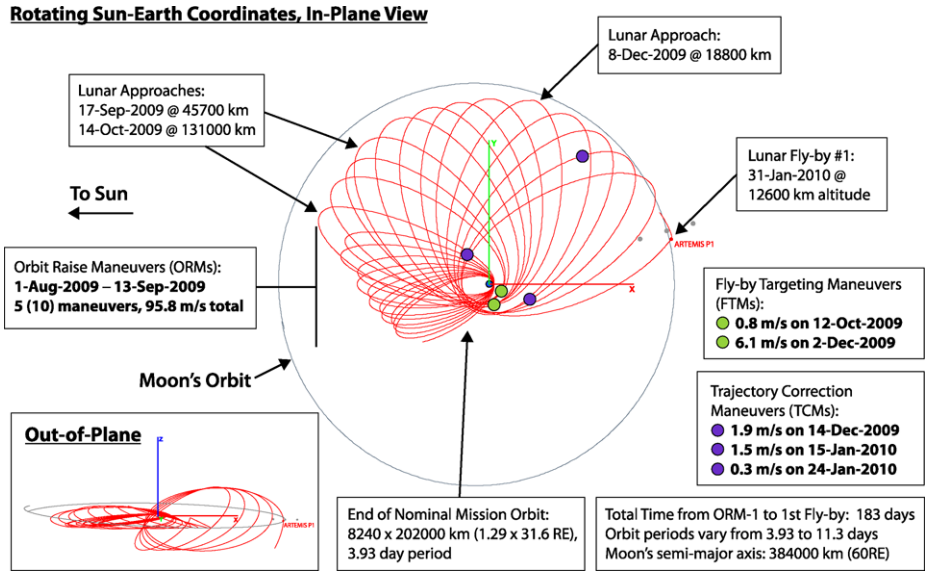


Fig. 4 Earth orbit portion of the P1 trajectory design. Distances quoted are ranges measured from the center of mass of the Earth or Moon

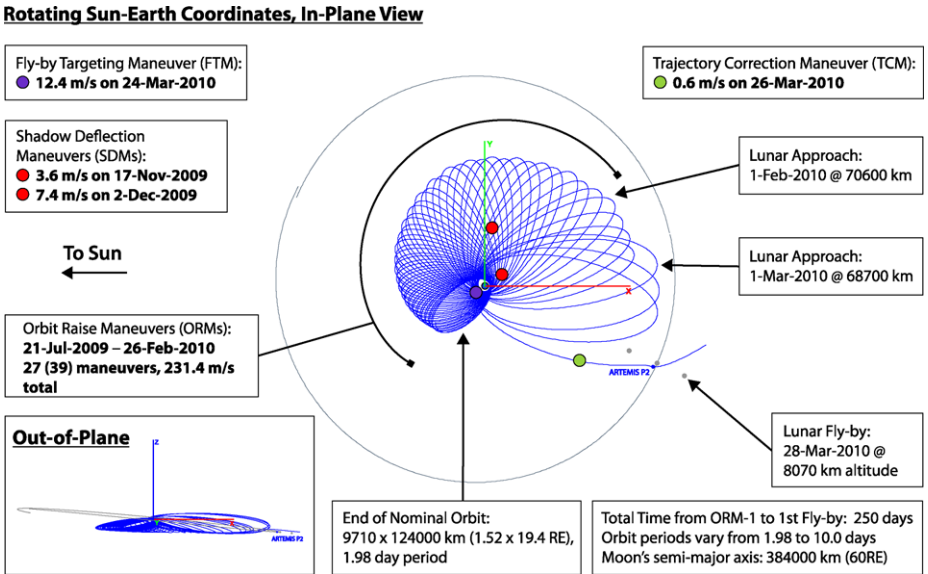


Fig. 5 Earth orbit portion of the P2 trajectory design. Distances quoted are ranges measured from the center of mass of the Earth or Moon

During the refinement of the orbit design, it was recognized that several factors conspired to further complicate the development of the reference trajectory:

1. Earth's shadow covers perigee for much of the orbit raise season, prohibiting thrusting at/near perigee. The design necessitated splitting most perigee burns into two (A and B) burn arcs bracketing the shadow, further increasing burn arc length and gravity losses.

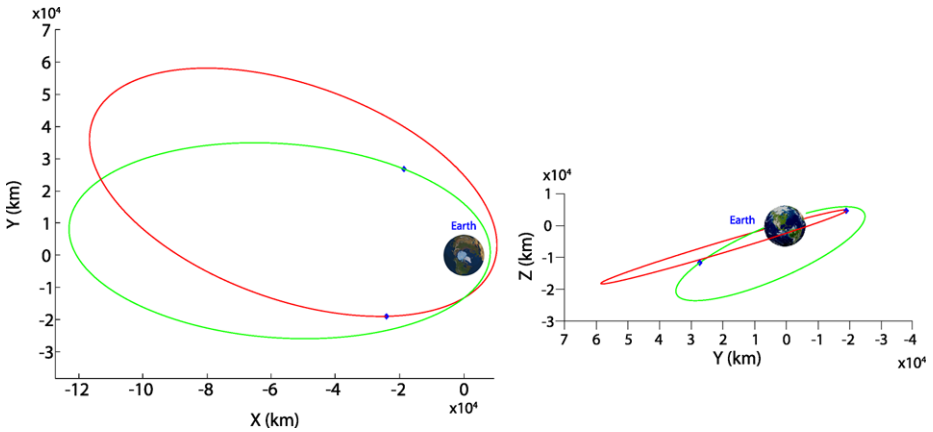


Fig. 6 (a) Initial orbit of the Earth orbit portion of the P1 preliminary trajectory design. The initial condition for ARTEMIS P1 predicted when ARTEMIS was proposed is in *green*; the actual starting orbit is in *red*. (b) End-on view of (a)

2. The initial propellant load of $\sim 50\%$ for P2 forced a large fraction of the maneuvers to be performed at a lower duty cycle (shorter pulse) due to the propellant load being near a “slosh resonance” (Sholl et al. 2007; Auslander et al. 2008; Frey et al. 2008). This further exacerbated gravity losses, necessitating more maneuvers to obtain the same total orbit-raise ΔV . This was addressed by starting the ORM sequence for P2 as early as July 20, 2009.
3. Side thrusting for orbit-raise maneuvers also results in a small reorientation (precession) of the spin axis due to a small offset of the thrust direction relative to the probe center of mass. The cumulative effect of side thrusting has been significant spin-plane precession of the probes in directions that either violated operational constraints or increased losses from vector-thrusting. Spin axis reorientation maneuvers were included in the mission design to account for that effect.
4. Thrust restrictions due to the absence of “up” thrusting capability posed a non-traditional restriction to the mission design. The usual intuition that 1 burn allows targeting of 3 elements and 2 burns separated in time allows for the targeting of 6 elements is not correct for ARTEMIS. In fact, even 3 separated burns can fail to provide 6-element targeting when all maneuvers are confined to a single plane.

5.1.1 Orbit-Raise Design Process

The P1 and P2 orbit-raise designs were constructed using Mystic software (Whiffen 1999; Whiffen 2006). Mystic was able to accommodate all mission constraints outlined above. However, the complex (and often treacherous) design space resulting from numerous lunar approaches during the orbit-raise phase made simple design strategies impossible. To provide some robustness against missed burns, and sufficient tracking data for orbit/maneuver reconstruction, perigee maneuvers were double-spaced, i.e., two orbits apart. On occasion it proved advantageous to separate burns even farther to take advantage of or avoid strong lunar interactions. Most perigee burns were divided into and modeled as two separate burn arcs, one on either side of the Earth’s shadow. The duration and pointing of each burn was

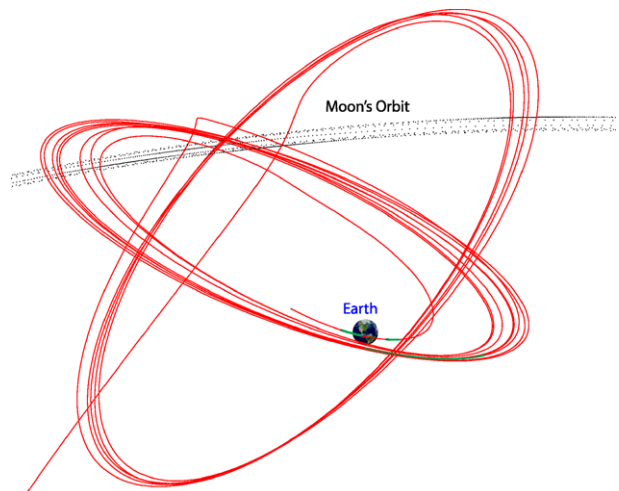
fully optimized using Mystic, with the constraint that the end states of this phase would be on the translunar trajectories already designed.

Several different end-to-end orbit-raise strategies were thus attempted for both P1 and P2, with the desired translunar injection as a goal and the initial ARTEMIS state as a starting point as early as needed, i.e., with an ascend start date unrestricted by THEMIS science considerations. The strategy that proved most successful for the P1 trajectory was to first optimize sets of burns on three double-spaced perigees to reach an orbital period of 131 hours. From states near this point forward, there existed a tremendous number of possible paths involving differing lunar interactions, numbers of Earth revolutions, plane changes, and node changes over the next 140 days of ballistic propagation. It was not at all obvious which of these many paths might be feasible, and then which feasible path would be best to rejoin the low-energy transfer. To address this problem, a large number of ballistic trajectories were used as initial guesses for targeting and optimization. Different families were organized based on the number of Earth revolutions. A computer cluster was used for this compute-intensive process. Trajectories that were found to be feasible or nearly feasible were then further refined by moving the time of rejoining the low-energy transfer to successively later dates.

5.1.2 P1 and P2 Orbit-Raise Designs

The P1 low-energy transfer began with a pair of lunar flybys separated by only 14 days—see Figs. 7 and 8. To minimize the ΔV cost of getting onto the designed translunar trajectory, it seems desirable to match these flybys as closely as possible, though exact matching does not seem to be necessary. Intuitively, re-joining the low-energy transfer at later times would provide increasing efficiency, since a longer time would allow a lower rendezvous velocity. It was expected (and found) that re-joining much beyond the second lunar flyby provided diminishing returns. The final total effective ΔV for P1's Earth orbit phase as actually flown was 102.7 m/s (compare this to the 103.7 m/s allocation (see Table 2) and the 125 m/s conservative estimate in the ARTEMIS proposal (Angelopoulos and Sibeck 2008) from a single-impulse Earth departure, which included 24 m/s for gravity and steering losses and trajectory correction maneuvers (TCMs)). The final design maneuvers are given in Table 3,

Fig. 7 P1's final Earth orbits leading into the low-energy transfer, showing an oblique view of the final lunar approach (which changed the orbit inclination significantly) and the first of the two lunar flybys that initiated the transfer. The *green arcs* along two of the orbit periapses show where the flyby targeting maneuvers (FTM1A, FTM1B, and FTM2) were performed



Rotating Sun-Earth Coordinates, In-Plane View

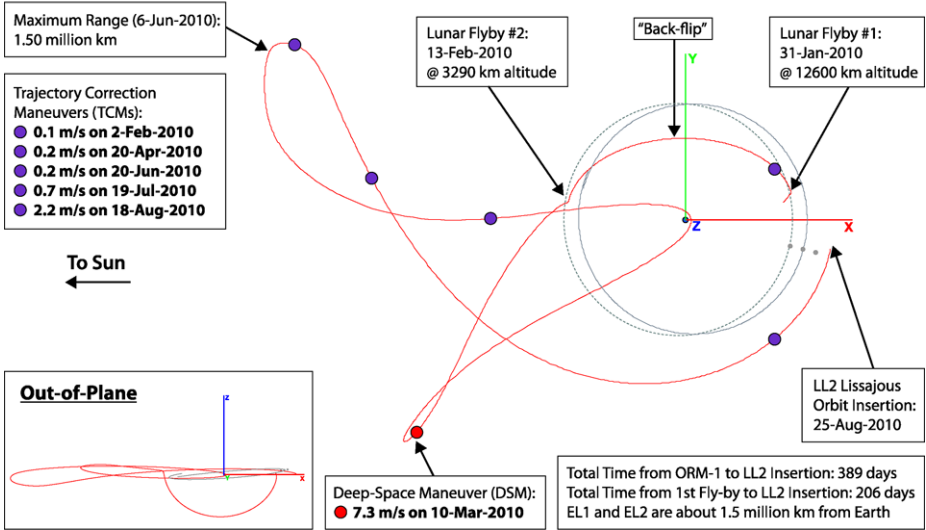


Fig. 8 Trans-lunar portion of the P1 trajectory design. Distances quoted are ranges measured from the center of mass of the Earth or Moon

along with trajectory correction maneuvers designed by the mission operations team during the execution of this phase.

The P2 orbit design was more complex than the P1 design because P2 begins in a much smaller orbit. A process similar to the P1 design process was used to develop the P2 orbit-raise design. Very careful planning of distant lunar approaches was necessary to stay within the allocated ΔV budget, which was more constraining for P2 than for P1. The P2 orbit raise required 42 burns, counting each split maneuver as two burns (see Table 4). The method used was a branching process. Each orbit-raise maneuver was designed several times to reach different orbital periods (different period = different “branch”). Subsequent maneuvers reaching longer periods were designed for each branch. The most promising branches were continued; poorly performing branches were abandoned. Poorly performing branches often led to situations in which lunar interactions reduced the orbit period or required long periods without maneuvers to avoid disadvantageous lunar interactions. Highly performing branches ended up with advantageous distant lunar interactions early on. Distant lunar interactions that provided maneuver savings as little as 1 meter per second early in the orbit raise were sought. The final few orbit-raise maneuvers required very careful planning to maximize the positive influence of the Moon.

A major additional complication of the P2 trajectory design occurred shortly before the first ORM, when a check for eclipses found an unacceptably long passage through Earth’s shadow just after the ORMs and before the first lunar flyby. Additional shadow-deflection maneuvers (SDMs) were added to change the orbit plane to reduce the time in shadow and then change the orbit plane back to return to the planned flyby conditions. These SDMs solved the problem without requiring a complete redesign of the series of ORMs, though at a cost of 11 m/s in additional ΔV . Even with these maneuvers added, the final total effective ΔV for P2’s Earth orbit phase as actually flown was 254.8 m/s (compare to the 245.7 m/s allocated and the 219 m/s originally estimated (Angelopoulos and Sibeck 2008) from the

Table 3 P1 Earth orbit and transfer phase maneuvers

ORM1A	2009/213	20:01:04.853	8.243
ORM1B	2009/213	20:50:51.171	8.441
ORM2A	2009/222	13:01:15.050	8.389
ORM2B	2009/222	13:51:33.867	8.468
ORM3A	2009/232	07:06:30.159	8.477
ORM3B	2009/232	07:56:36.098	8.517
ORM4A	2009/243	08:12:29.465	13.901
ORM4B	2009/243	09:14:21.187	11.855
ORM5A	2009/256	18:57:06.519	13.984
ORM5B	2009/256	19:48:19.402	5.505
FTM1A	2009/285	08:38:00.635	0.203
FTM1B	2009/285	08:41:51.037	0.602
FTM2	2009/336	08:02:21.215	6.084
TCM1	2009/348	04:51:56.825	1.886
TCM2	2010/015	12:27:38.304	1.455
TCM3	2010/024	07:00:59.591	0.311
TCM4	2010/033	07:10:53.521	0.116
DSM1	2010/069	19:00:00.000	7.312
TCM5	2010/110	09:00:00.000	0.179
TCM6	2010/171	21:45:00.000	0.180
TCM7	2010/200	23:00:00.000	0.651
TCM8	2010/230	06:00:00.000	2.244

single-impulse Earth departure, which included 33 m/s for gravity and steering losses and TCMs). The final design and trajectory correction maneuvers are given in Table 4.

5.2 Trans-lunar Phase Trajectories

The trans-lunar phase of the ARTEMIS trajectory for each probe extended from the first close lunar flyby to insertion into the target Lissajous orbit.

Figure 8 shows the trans-lunar phase of the ARTEMIS trajectory for P1. The trajectory is shown in the same Sun-Earth synodic coordinate frame used in Figs. 4 and 5. In the figure the trajectory begins on the right side of the plot with “Lunar Fly-by #1”. The P1 trajectory made use of a “back-flip”, wherein the first lunar fly-by set up a second lunar fly-by on the opposite side of the Moon’s orbit ~ 14 days later. The back-flip can be seen clearly in the out-of-plane view insert in the bottom left of Fig. 8 and the beginning of it is shown in Fig. 7. This second flyby raised the apogee significantly, throwing the probe out beyond the Moon’s orbit towards the Sun. This began the low-energy trajectory leg for P1, which is characterized by significant gravitational perturbation imparted on the probe by the Sun. This low-energy trajectory had two deep-space legs that included one relatively small deep-space maneuver (DSM). After the second leg, the orbit perigee had been raised to lunar distance, and the phasing with the Moon’s orbit was such that the probe moved into a lunar Lissajous orbit around lunar Lagrange point #2 (LL2) without requiring any deterministic insertion maneuver. By the time P1 reached the Lissajous orbit in August of 2010, 389 days had elapsed since the start of ARTEMIS maneuver operations.

Figure 9 shows the trans-lunar trajectory for P2. The P2 trajectory only included one lunar fly-by, which sent the probe away from the Sun and beyond the Moon’s orbit into a

Table 4 P2 Earth orbit and transfer phase maneuvers

ORM1	2009/202	07:33:03.552	10.686
ORM2	2009/206	10:41:40.407	5.292
ORM3A	2009/210	15:10:44.501	2.399
ORM3B	2009/210	16:10:50.116	8.348
ORM4A	2009/215	00:46:49.019	3.324
ORM4B	2009/215	01:47:36.747	8.695
ORM5A	2009/219	15:24:58.115	3.870
ORM5B	2009/219	16:22:13.277	7.915
ORM6A	2009/224	11:22:18.944	3.903
ORM6B	2009/224	12:16:13.013	6.952
ORM7A	2009/229	12:35:08.258	3.867
ORM7B	2009/229	13:26:36.035	6.257
ORM8A	2009/234	19:27:11.635	4.267
ORM8B	2009/234	20:18:08.362	6.058
ORM9A	2009/240	08:07:08.656	3.871
ORM9B	2009/240	08:53:50.173	4.753
ORM10A	2009/246	02:16:11.659	4.729
ORM10B	2009/246	03:01:38.535	4.387
ORM11A	2009/252	02:39:19.201	5.000
ORM11B	2009/252	03:21:47.856	3.419
ORM12A	2009/258	09:02:17.385	5.586
ORM12B	2009/258	09:43:04.698	2.831
ORM13A	2009/264	22:31:20.114	5.882
ORM13B	2009/264	23:11:39.983	2.507
ORM14A	2009/271	18:34:32.874	7.092
ORM14B	2009/271	19:14:07.763	2.240
ORM15	2009/278	23:21:22.389	5.881
ORM16	2009/286	09:49:58.506	8.599
ORM17	2009/294	06:15:08.345	9.851
ORM18	2009/302	13:41:36.289	10.269
ORM19	2009/311	10:47:56.571	10.113
ORM20	2009/320	22:41:23.999	10.039
ORM21	2009/331	01:50:58.997	4.148
ORM22	2009/341	12:28:02.607	2.083
ORM23	2009/352	07:22:49.060	4.782
ORM24	2009/363	11:22:37.941	6.233
ORM25	2010/010	05:05:57.689	7.580
ORM26	2010/022	19:08:17.058	5.846
ORM27	2010/057	08:52:20.815	11.875
SDM1	2010/059	08:17:18.815	3.636
SDM2	2010/074	09:55:42.965	7.360
FTM1	2010/083	16:07:17.000	12.406
TCM1	2010/085	02:05:41.282	0.648
DSM1	2010/133	02:21:16.534	3.685
DSM2	2010/152	14:50:00.000	23.280
TCM2	2010/201	12:00:00.000	2.152
TCM3A	2010/214	11:58:28.326	0.634
TCM3B	2010/214	12:01:37.625	0.090
DSM3A	2010/252	13:58:24.982	2.478
DSM3B	2010/252	14:01:59.393	0.797
TCM4	2010/274	11:00:00.000	0.306
TCM5	2010/285	13:40:00.000	0.250

Rotating Sun-Earth Coordinates, In-Plane View

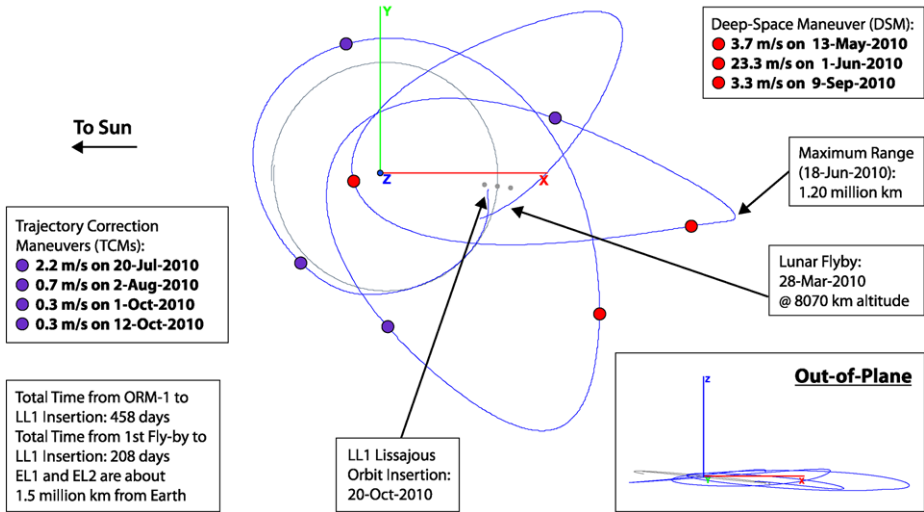


Fig. 9 Trans-lunar portion of the P2 trajectory design. Distances quoted are ranges measured from the center of mass of the Earth or Moon

region where the perturbative influence of solar gravity is significant. P2 followed a low-energy trajectory that included three deep-space legs before entering a lunar Lissajous orbit around lunar Lagrange Point #1 (LL1) without any deterministic thrusting. The P2 trajectory included three deep-space maneuvers (DSM), one of which was relatively large; these maneuvers totaled 30.4 m/s. P2 arrived in Lissajous orbit about 2 months after P1, requiring a total of 458 days since the start of ARTEMIS maneuver operations to reach this stage.

5.2.1 Transfer Trajectory Implementation

As the transfer trajectory was flown, correction maneuvers were required to adjust for earlier maneuver execution and probe pointing and implementation errors, as well as navigation errors. These maneuvers, called trajectory correction maneuvers (TCMs), encompassed the statistical maneuvers along the transfer. TCMs in addition to DSMs were inserted in each of the P1 and P2 designs.

We allocated 4% of the total propellant budget of each probe to perform any required TCMs along the way to control the energy to keep P1 and P2 near their appropriate outgoing trajectories. Since the two probes had already completed their primary mission in a highly elliptical Earth orbit, propellant was extremely limited. Thus, with the unique operational constraints, accomplishment of the transfer goals with the minimum propellant cost was the highest priority. To implement the mission design, our trajectory simulations use a full ephemeris model with point-mass gravity representing Earth, Moon, Sun, Jupiter, Saturn, Venus, and Mars. Also included is an eighth degree and order Earth potential model. The solar radiation pressure force is based on: (1) the measured probe area, (2) the probe estimated mass (from bookkeeping), and (3) the coefficient of reflectivity determined by navigation estimation. The same models with estimates for the mass usage and coefficient of reflectivity were used in the mission design process that determined the reference trajectory. The trajectory propagations in operations were based on a variable step Runge-Kutta

8/9 and Prince-Dormand 8/9 integrator. Initial conditions used throughout the planning process correspond to the UCB-delivered navigation solutions using the DSN and the UCB tracking system. Software tools used in this process include the General Mission Analysis Tool (GMAT) developed at GSFC as an open source, high-fidelity tool with optimization and MATLAB connectivity and AGI's STK/Astrogator suite.

To compute actual commanded maneuver ΔV requirements, we used two numerical methods: differential corrections (DC) targeting using central or forward differencing and an optimization method using the VF13AD algorithm from the Harwell library. A DC process provided *a priori* conditions. Equality constraints were incorporated for DC application; nonlinear equality and inequality constraints were employed for optimization. These constraints incorporated both the desired target conditions in the Earth-Moon system and probe constraints on the ΔV direction and relationship between the spin axis and the ΔV vector.

The end goal of the transfer phase was to achieve the Earth-Moon Lissajous insertion conditions necessary for a minimal energy insertion into the Earth-Moon L2 or L1 Lissajous orbits. The goals were defined in terms of states expressed in Earth J2000 coordinates. These targets were held constant over the entire mission design and implementation process once the reference translunar transfer had been designed. Although a baseline trajectory was defined to design the mission, the adaptive strategy used in operations required exactly matching this baseline only at the end of the transfer.

5.2.2 Navigation Uncertainties

Throughout the transfer trajectory implementation process, navigation solutions were generated at a regular frequency of once every three days with the exception of post-maneuver navigation solutions, which were made available as soon as a converged solution was determined. The rapid response was to ensure that the maneuver had performed as predicted and that no unanticipated major changes to the design were necessary. The RSS of the uncertainties were on the order of tens of meters in position and below 1 cm/s in velocity. As a conservative estimate for maneuver planning and error analysis, 1σ uncertainties of 1 km in position and 1 cm/s in velocity were used. These accuracies were obtained using nominal tracking arcs of one three-hour contact every other day. The Goddard Trajectory Determination System (GTDS) was used for all navigation estimations.

5.2.3 Trajectory Design During Operations

The transfer trajectory implementation approach used the numerical methods discussed above augmented by dynamical systems theory for verification and to gain knowledge of the transfer dynamics. The probes were targeted to the libration point orbit insertion locations knowing full well that maneuver execution and navigation errors would push the path off the "baseline" design. A correction maneuver scenario was planned that would essentially shift the trajectory, such that the new path would be consistent with a nearby manifold. It was decided to use a forward-integrating numerical optimization process that included probe constraints to calculate optimized ΔV s. This procedure permitted minimization of the ΔV magnitude, variation of the ΔV components in direction, as well as variation of the maneuver epoch, while incorporating the nonlinear constraint on the probe ΔV direction relative to the spin axis.

Originally, it was envisioned that errors in navigation and maneuvers could lead to the need for an unobtainable correction in an "up" direction with respect to the ecliptic plane. Fortunately, experience with trajectory design on other missions that incorporate weak stability regions near Sun-Earth libration orbits and near the ecliptic plane showed us that we

could allow upward ΔV corrections to be delayed until an equivalent magnitude but opposite direction (downward) ΔV location could be found in the long-duration transfer. These locations were then used to correct the trajectories without any upward maneuver component to achieve the final Earth-moon insertion targets.

As the TCMs were performed, the path essentially jumped from the vicinity of one local transfer manifold to another at a slightly different energy level. The number of optimized TCMs was very low and their magnitudes quite small, considering the sensitivity of the dynamics and uncertainties of the OD solutions.

5.2.4 Maneuver Design

To target to the desired Earth-Moon Lissajous conditions, a VF13AD optimizer was used. We optimized each maneuver to determine the minimal ΔV location. To determine an *a priori* maneuver location and to achieve an intuitive feel for the maneuver results, a DC process was first performed using planned DSN coverage. For P1, the first four TCMs were completed in Earth-centered elliptical orbit or during lunar gravity-assist targeting. Maneuver execution errors are small, only a few percent. These errors are a function of actual start time with respect to a sun pulse of a spinning spacecraft, tank temperatures, attitude knowledge, and general propulsion system performance.

It should be noted that maneuver execution errors, current navigation errors, and subsequent maneuvers to correct for these errors along with small mis-modeled perturbations can lead not only to late or early arrival times at the prescribed Lissajous insertion location, but also may contribute to out-of-plane effects and may result in trajectories that intersect with the Moon. Clearly, the trajectory is very sensitive to such small variations. But that sensitivity also implies that small corrections can alter the trajectory design significantly and allow low ΔV cost orbit control, assuming sufficiently frequent tracking for orbit reconstruction.

5.3 Lissajous Orbit Phase Trajectories

The Lissajous orbit phase of ARTEMIS has permitted repeated observations of the distant lunar wake. For the first ~ 1.5 months of this phase (from August 22 to October 2, 2010), P1 was alone at the Moon in orbit around the LL2 point while P2 was still en route. P2 then arrived, making a partial orbit around LL2 on its way to Lissajous orbit at LL1. For about the next 2.3 months, P1 orbited LL2 while P2 orbited LL1, and then P1 also crossed over to orbit LL1. During this phase, the trajectories permit 16 independent observations of the lunar wake when crossing behind the Moon on the anti-Sun side, observations of the distant Earth magnetotail once per month when the Moon's orbit passes through it, and observations of the pristine solar wind when out of the influence of both. These two-point measurements were made at separation scales up to $\sim 100,000$ km when the probes were in orbit around different Lagrange points and up to $\sim 50,000$ km when both orbit LL1. Distant magnetotail measurements can also be correlated with concurrent measurements from THEMIS-A, THEMIS-D, and THEMIS-E in low-Earth orbit.

Figure 10 shows the P1 trajectory during the Lissajous orbit phase. In this figure, the Moon is at the origin and the trajectory is drawn in the Earth-Moon synodic coordinate frame, which rotates such that the Earth is always to the left along the negative X axis. The Z axis is aligned with the angular momentum vector of the Moon's geocentric orbit. The main figure on the left side shows the view looking down on the geocentric orbital plane of the Moon, and the two insets show perspectives from within the Moon's orbital plane. The LL1 and LL2 points are marked in the figure.

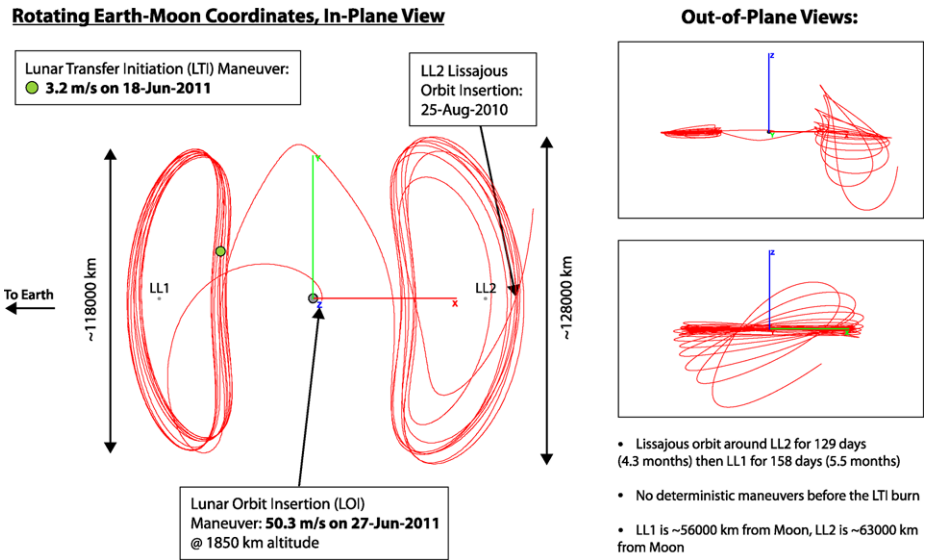


Fig. 10 Lissajous orbit phase of the P1 trajectory. Distances given are ranges measured from the lunar center of mass unless otherwise specified

P1 entered Lissajous orbit around LL2 on August 25, 2010 with only a stochastic maneuver to begin station-keeping. Although the initial Lissajous orbit was somewhat inclined with respect to the Moon’s geocentric orbit plane, the orbit flattened after a few orbits (see Fig. 10 inserts). After ~129 days in orbit around LL2, P1’s trajectory followed an unstable orbit manifold along a 10-day heteroclinic connection to a Lissajous orbit around LL1 (Howell et al. 1997; Koon et al. 2000). Although this transfer required no deterministic ΔV for initiation or insertion, in practice weekly station-keeping maneuvers (SKMs) were required to maintain the Lissajous orbit. P1 spent 158 days orbiting LL1 before executing a small maneuver to depart from Lissajous orbit on June 18, 2011. The probe descended to an 1850 km periselene altitude, where the lunar-orbit insertion (LOI) maneuver was executed, beginning the lunar orbit phase on June 27, 2011. At the time of LOI, P1 had operated for 707 days since the beginning of the ARTEMIS mission.

Figure 11 shows the P2 trajectory during the Lissajous orbit phase. P2 entered Lissajous orbit around LL1 on October 20, 2010. As with P1, this insertion was achieved without any deterministic ΔV because the incoming trans-lunar trajectory approached on the stable manifold of this particular Lissajous orbit. P2 stayed in this nearly planar Lissajous orbit for about 8.5 months before initiating descent to a ~3800 km altitude periselene. The LOI maneuver for P2 occurred on July 17, 2011, at which time P2 had been operating for 727 days since the end of the nominal THEMIS mission.

After P1 and P2 entered their Lissajous orbits, a project decision was made to extend the Lissajous phase from April to July. This required adding axial components to SKM18 on February 1, 2011, for P1 and to SKM11 (January 4), SKM13 (January 18), and SKM15 (February 1) for P2. These axial burns, which directly affected the Z velocity of the probes in the Earth-Moon frame, were needed to prevent the Z axis components of the Lissajous orbit states from oscillating too much. These oscillations otherwise would have grown to uncontrollable levels before the transition to lunar orbits despite ARTEMIS’s stationkeeping process.

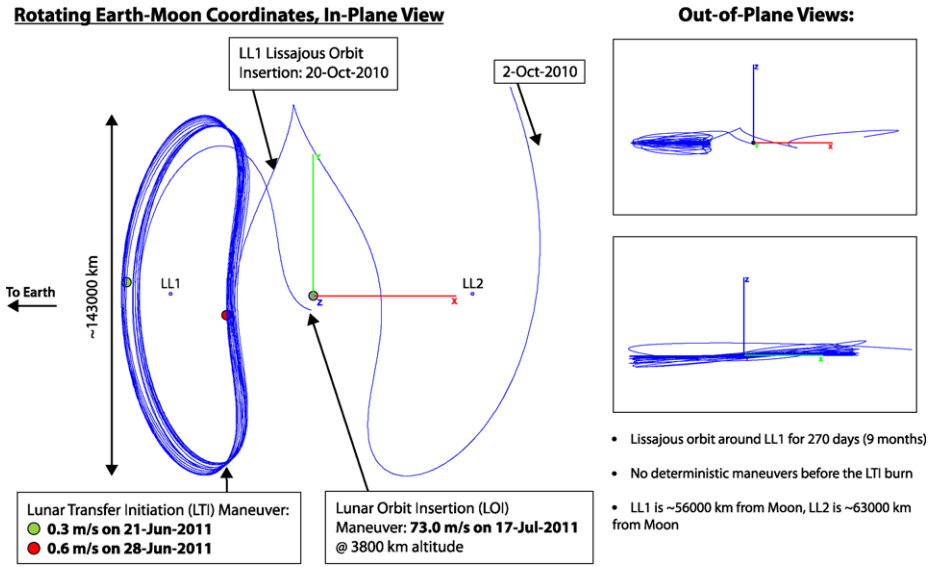


Fig. 11 Lissajous orbit phase of the P2 trajectory design. Distances given are ranges measured from the lunar center of mass unless otherwise specified

The Lissajous orbit phase of the ARTEMIS mission were particularly exciting because the ARTEMIS probes are the first to fly in a lunar Lissajous orbit. Flying these orbits was a challenge for operations and maneuver design teams because Lissajous orbits are inherently very unstable; small, unavoidable deviations from the Lissajous orbit are amplified to problematic proportions (Howell and Keeter 1995) after approximately one revolution (~14 days). This leaves little room for error in the operations. Because of this instability, correction maneuvers needed to be executed about weekly to keep the probes in orbit. So even though these orbits required no deterministic ΔV , orbit maintenance ΔV was required.

5.3.1 Stationkeeping

There are many stationkeeping methods to choose from: classical control theory or linear approximations of Farquhar (1971), Farquhar and Kamel (1973), Breakwell and Brown (1979), and Hoffman (1993), provided analysis and discussion of stability and control in the Earth-Moon collinear L1 and L2 regions; Renault and Scheeres (2003) offered a statistical analysis approach; Howell and Keeter (1995) addressed the use of selected maneuvers to eliminate the unstable modes associated with a reference orbit; and Gómez et al. (1998) developed and applied the approach specifically to translunar libration point orbits. Folta et al. (2010) presented an analysis of stationkeeping options and transfers between the Earth-Moon locations and the use of numerical models that include discrete linear quadratic regulators and differential correctors.

The ARTEMIS stationkeeping method used maneuvers performed at optimal locations to minimize the ΔV requirements while ensuring continuation of the orbit over several revolutions downstream. There are no reference trajectories to plan against, so other methods such as linear (continuous) controllers are impractical. Likewise, other targeting along the X axis or Y axis is more costly or cannot be attained without violating probe constraints. Goals in the form of energy achieved, velocities, or time at any location along the orbit

can be used, but our goal was defined in terms of the X velocity component at the X axis crossings. This assumes selection of a velocity that can be related to the orbit energy at any particular time. To initialize the analysis, a DC scheme is used, based on the construction of an invertible sensitivity matrix by numerical sampling of orbital parameters downstream as a consequence of specific initial velocity perturbations (Folta et al. 2010). The orbit is continued over several revolutions by checking the conditions at each successive goal then continued to the next goal. This allows perturbations to be modeled over multiple revolutions.

The targeting algorithm uses an impulsive maneuver with variables of either Cartesian ΔV components or ΔV magnitude and azimuth angle within the ARTEMIS spin plane. Target goals are specified uniquely for each controlled orbit class because LL1 and LL2 dynamics differ slightly. The velocity target chosen is specifically set to continue the orbit in the proper direction. Targeting is then implemented with parameters assigned at the X – Z plane crossing such that the orbit is balanced and another revolution is achieved. Each impulsive maneuver is targeted to the X component of the velocity at the third X axis crossing after the maneuver; the maneuver supplies velocity (energy) in a direction that subsequently continues the libration point orbit. Additionally, the VF13AD1 optimizer is used to minimize the stationkeeping ΔV by optimizing the direction of the ΔV and the location (or time) of the maneuver. Included in the DC and optimization process are constraints required to keep the ARTEMIS maneuvers in the spin plane.

Given the constraints of the ARTEMIS mission orbit, probe maneuvers were planned at a seven-day frequency to ensure a stable navigation solution while minimizing the ΔV s and staying within the ARTEMIS ΔV budget. The maneuvers were originally planned to occur at or near the X axis crossings and to use a continuation method to maintain the orbit. As operational experience was gained, however, it was found possible to relax the location of each maneuver in order to permit a more user-friendly operational schedule. Orbital conditions were set to permit the energy or velocity at the crossings to continue the orbit for at least 2 revolutions.

Since oscillations in the Z component of the state are largely decoupled from motion in the X – Y plane and are not as unstable as that motion, our expectation was that these oscillations could be controlled using maneuvers only in the probes' $+Z$ directions, which were close to ecliptic south for each probe; this proved to be the case for this oscillation control (described earlier in this section) as well as for statistical Z control throughout the Lissajous phase. The complete set of stationkeeping maneuvers for both probes is detailed in Tables 5 and 6.

5.4 Lunar Orbit Phase Trajectories

Most scientific observations for ARTEMIS occur during the lunar orbit phase, which nominally lasts 2 years. It was desirable for the lunar orbit to have apoapsis as high as possible in order to enable a large range of downstream lunar wake measurements. Another goal for the mission was to maximize the number of periapses less than 50 km altitude in order to best measure crustal magnetism and sputtered ions. Long orbit lifetimes and at least some inclination relative to the lunar equator would help to maximize the variety of measurement opportunities. Considering also the spacecraft capabilities, the ARTEMIS lunar orbits were chosen to have apoapsis radius around 19,000 km (driven by the maximum acceptable eclipse duration) with periapsis altitudes varying between roughly 20 and 1200 km altitude. The P1 orbit is retrograde with a lunar periapsis latitude range of ± 12 deg and the P2 orbit is prograde with a periapsis latitude range of ± 17 deg.

Table 5 P1 Lissajous maneuvers

SKM1	2010/237	04:30:00.000	2.562
SKM2	2010/251	11:00:00.000	0.584
SKM3	2010/265	09:00:00.000	0.223
SKM4	2010/273	16:25:00.000	0.341
SKM5	2010/282	16:30:00.000	0.078
SKM6	2010/291	14:00:00.000	0.158
SKM7	2010/298	07:00:00.000	0.113
SKM8	2010/306	05:00:00.000	0.116
SKM9	2010/313	01:45:00.000	0.066
SKM10	2010/321	08:45:00.000	0.072
SKM11	2010/334	05:55:00.000	0.210
SKM12	2010/344	06:30:00.000	0.227
SKM13	2010/352	14:30:00.000	0.139
SKM14	2010/361	17:15:00.000	0.117
SKM15	2011/006	18:40:00.000	0.033
SKM16	2011/017	06:55:00.000	0.120
SKM17	2011/024	08:00:00.000	0.062
SKM18A	2011/032	18:35:00.000	2.100
SKM18B	2011/032	18:45:00.000	0.192
SKM19	2011/038	19:05:00.000	0.224
SKM20	2011/045	06:10:00.000	0.104
SKM21	2011/049	20:45:00.000	0.014
SKM22	2011/056	04:20:00.000	0.060
SKM23	2011/063	00:00:00.000	0.030
SKM24	2011/070	03:45:00.000	0.029
SKM25	2011/076	10:25:00.000	0.017
SKM26	2011/083	02:35:00.000	0.023
SKM27	2011/089	19:10:00.000	0.020
SKM28	2011/096	18:55:00.000	0.019
SKM29	2011/103	10:30:00.000	0.022
SKM30	2011/110	02:00:00.000	0.281
SKM31	2011/116	16:45:00.000	0.029
SKM32	2011/124	14:15:00.000	0.130
SKM33	2011/131	07:20:00.000	0.061
SKM34	2011/144	15:55:00.000	0.056
SKM35	2011/150	20:40:00.000	0.012
SKM36	2011/157	19:40:00.000	0.043
SKM37/LTI	2011/169	00:31:00.000	3.229
SKM38/LTI-TCM1	2011/173	01:00:00.000	0.509

The conic orbit elements of these lunar orbits are subject to constant change primarily induced by Earth's perturbing gravitational influence during the high apoapses. In the lunar orbit phase, periapsis altitudes vary by 800–1000 km twice per lunar orbit around the Earth (i.e., roughly every two weeks) due to tidal forces. Because the Earth's location relative to the Moon's surface is nearly fixed, this two week oscillation in periapsis altitude always has a minimum near the same lunar longitudes: 90 deg and 270 deg for a retrograde orbit (P1)

Table 6 P2 Lissajous phase maneuvers

SKM1	2010/293	12:50:00.000	0.117
SKM2	2010/300	06:15:00.000	0.184
SKM3	2010/307	14:05:00.000	0.379
SKM4	2010/315	10:50:00.000	0.247
SKM5	2010/322	05:25:00.000	0.063
SKM6	2010/333	04:45:00.000	0.350
SKM7	2010/340	22:55:00.000	0.104
SKM8	2010/348	03:40:00.000	0.066
SKM9	2010/355	12:40:00.000	0.036
SKM10	2010/362	16:25:00.000	0.122
SKM11	2011/004	16:42:00.000	0.960
SKM12	2011/011	20:40:00.000	0.120
SKM13	2011/018	13:45:00.000	0.170
SKM14	2011/025	10:05:00.000	0.177
SKM15A	2011/032	02:10:00.000	0.030
SKM15B	2011/032	02:15:00.000	0.038
SKM16	2011/039	08:35:00.000	0.294
SKM17	2011/050	02:20:00.000	0.173
SKM18	2011/057	17:00:00.000	0.036
SKM19	2011/065	05:50:00.000	0.216
SKM20	2011/072	22:30:00.000	0.211
SKM21	2011/079	10:45:00.000	0.044
SKM22	2011/086	20:30:00.000	0.020
SKM23	2011/100	20:10:00.000	0.050
SKM24	2011/107	10:55:00.000	0.045
SKM25	2011/116	10:25:00.000	0.017
SKM26	2011/123	17:30:00.000	0.068
SKM27	2011/130	18:35:00.000	0.023
SKM28	2011/138	02:05:00.000	0.019
SKM29	2011/143	17:05:00.000	0.014
SKM30	2011/151	00:05:00.000	0.024
SKM31	2011/161	04:00:00.000	0.068
LTI1	2011/172	01:00:00.000	0.347
LTI2	2011/179	16:15:00.000	0.622
LTI-TCM	2011/186	06:20:00.000	0.086

and 0 deg and 180 deg for a prograde orbit (P2). Another longer term eccentricity oscillation is induced by the secular precession of the argument of periapsis caused by the Earth for the ARTEMIS orbits (Scheeres et al. 2001). This oscillation causes periapsis altitudes to vary by a few hundred km every few months. The P1 and P2 periapsis altitudes through 2013 clearly show the influence of these two oscillations (Fig. 12).

Another effect of Earth's perturbation on the orbits is to cause the ecliptic longitude of the periapse for each orbit to change in the same direction as the orbital motion by about 100 deg per year. By putting the probes into opposing orbits, e.g., P2 prograde and P1 retrograde, the relative motion of their lines of apsides is maximized. The combination of this apsidal motion with the significant eccentricity of the orbits enables observations to be achieved at

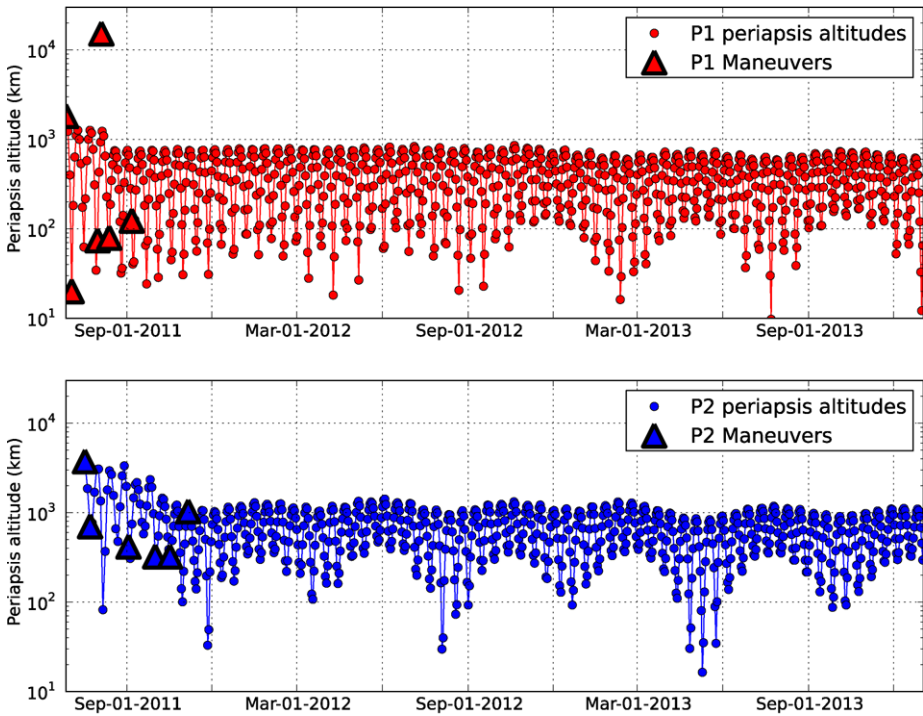


Fig. 12 Altitude at periapse for P1 and P2 in lunar orbit. The bi-weekly and every-few-monthly oscillations in periapsis altitude are clearly shown. Note that small PEB maneuvers are planned for 2012 and 2013 but are not explicitly labeled here

a wide range of probe separations (from ~ 150 to $\sim 30,000$ km) and geometries in the lunar wake.

5.4.1 Lunar Orbit Insertion and Achieving the Science Orbit

Achieving the ARTEMIS science orbits was a challenging problem due to the small size of the tangential thrusters, the limited ΔV available, and the aforementioned strong Earth perturbations. The approach trajectories from Lissajous orbit could not enter the science orbit with a single lunar orbit insertion (LOI) maneuver because not enough ΔV was available. It was necessary to divide the insertion into many maneuvers to reduce the gravity and steering losses to an acceptable level. The implemented transfer design consists of an LOI maneuver plus five period reduction maneuvers (PRMs) for each spacecraft. The geometries of the P1 and P2 approaches from Lissajous and subsequent transfers to the science orbit are shown in Fig. 13. The timing and ΔV of each maneuver, as executed, is given in Table 7.

The first steps toward achieving the science orbit were performed during the Lissajous orbit phase. An out-of-plane component was included in SKMs in January and February of 2011 that set the inclination of approach to LOI such that an acceptable science orbit inclination could be achieved. This method of inclination modification is very fuel efficient relative to a plane-change maneuver in lunar orbit.

Relatively large LOI maneuvers with significant gravity losses were required to capture P1 and P2 into a low enough orbit so that Earth-gravity perturbations did not result in impact

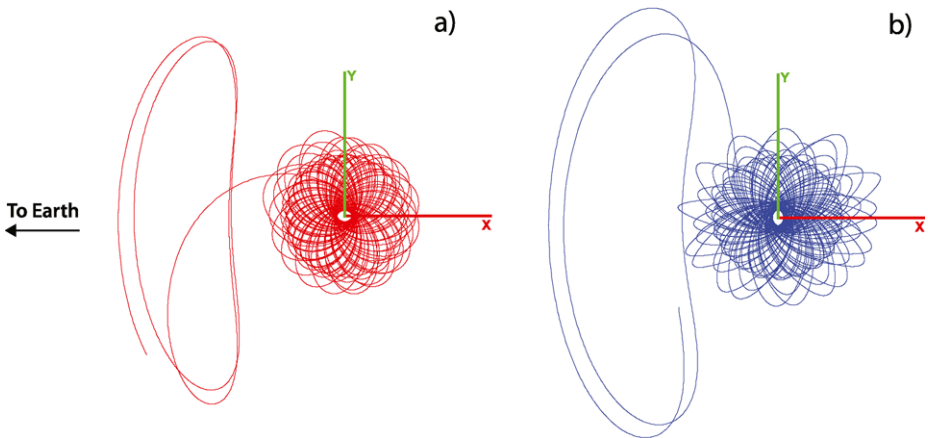


Fig. 13 LOI and low-lunar orbit trajectories for (a) P1 and (b) P2 in the rotating Moon-centered frame. LL1 Lissajous orbits shown for scale

Table 7 LOI and PRM maneuver details for both spacecraft in chronological order. It was an important design criterion that the activities on one spacecraft did not interfere with planning or execution of activities on the other. The total ΔV expended on these maneuvers was 91.1 m/s for P1 and 118.4 m/s for P2

Burn name	Date	Total ΔV (m/s)	# of segments
P1 LOI	June 27, 2011	50.3	3
P1 PRM-1	July 3, 2011	12.1	2
P2 LOI	July 17–18, 2011	73.0	3
P2 PRM-1	July 23, 2011	8.5	2
P1 PRM-2	July 31, 2011	4.6	1
P1 PRM-3	August 3, 2011	2.5	1
P1 PRM-4	August 12, 2011	13.0	2
P2 PRM-2	September 2, 2011	12.4	2
P1 PRM-5	September 7, 2011	8.6	1
P2 PRM-3	October 1, 2011	13.3	2
P2 PRM-4	October 17, 2011	7.7	2
P2 PRM-5	November 7, 2011	3.5	1

on subsequent periapses. The geometry to the approach from Lissajous orbit determines the initial phasing on the bi-weekly periapsis altitude oscillation and the magnitude of the oscillation grows with the apoapsis altitude. The approach phase was effectively fixed due to dynamics and the future objective to coordinating measurements with LADEE. Thus, to avoid impact at the minimum of the oscillation cycle, the LOI altitude had to be high enough and LOI duration long enough to avoid a surface-impacting post-LOI orbit. The P1 LOI altitude was selected to be 1850 km and the P2 LOI altitude was at 3800 km. At these altitudes, the minimum safe burn duration for LOI was 135 minutes for P1 and 173 minutes for P2 with the roughly 0.5 N thrust available at the time of LOI (assuming use of a ± 30 deg pulse width). The P2 LOI duration was further increased to 205 minutes to improve the eclipse phasing for the subsequent PRMs. Since the ARTEMIS thrust cannot be dynamically steered along an anti-velocity direction without significant redesign of its thruster operations software, the LOIs were divided into three constant-direction thrust segments in order to reduce steering losses; these segments were separated by a minimum of three minutes for operational reasons.

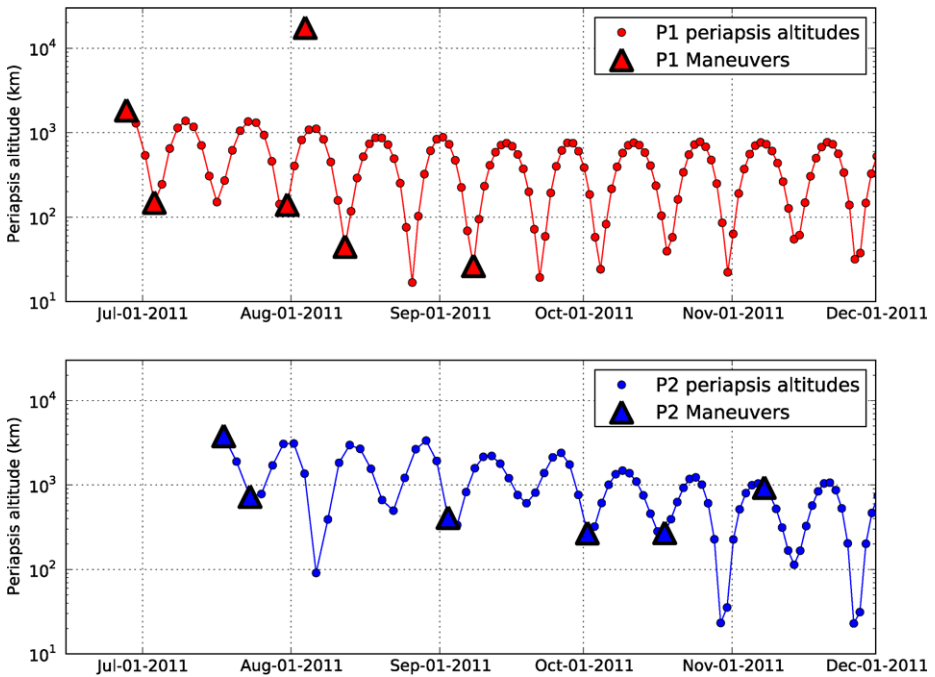


Fig. 14 Time history of periapsis altitudes for P1 and P2 during the first 6 months in orbit. LOI and PRM maneuver dates are marked as *triangles*. All maneuvers were roughly centered around periapsis with the exception of P1's PRM-3, which was at apoapsis

After a safe capture orbit was achieved with the LOI maneuvers, the rest of the transition to the science orbits was achieved with a series of smaller and more efficient PRM burns. For maximum fuel-efficiency, an infinite number of very small PRMs at periapses would be ideal. For ARTEMIS, a total of 10 PRMs (5 for each spacecraft) were performed over a period of 5 months. PRMs were included on periapse numbers 3, 20, 28, and 49 and apoapsis number 22 for P1. For P2, PRMs were placed at periapse numbers 2, 20, 36, 47, and 63. The placement of these PRM maneuvers relative to the bi-weekly periapsis altitude oscillation is shown in Fig. 14. A number of factors were considered in determining the placement and sizing of the PRM maneuvers including: ΔV efficiency (using the lowest periapsis altitudes is most efficient), operations schedule (sufficient time for orbit determination, maneuver design, and testing must exist between maneuvers), operations staff availability (P1 and P2 activities should not be simultaneous since a single team operates both spacecraft), orbit lifetime (should not be less than 14 days if a maneuver is missed), final stable orbit altitude (PRMs needed to manage periapsis altitudes to ensure a low altitude final orbit), eclipses (spacecraft cannot maneuver in eclipse and shadow times must be less than 4 hrs), occultations (flight rules prohibit maneuver initialization when out of radio contact), and the performance of preceding PRMs (the PRM sequence design was modified as needed after each maneuver execution). The total characteristic ΔV expended for execution of the combined LOI and PRMs was 91.1 m/s for P1 and 118.4 m/s for P2, where *characteristic ΔV* is the ΔV the thrusters would have provided if the spacecraft weren't spinning. Additional detail on the design of the transfer from Lissajous to the science orbit can be found in Broschart et al. (2011).

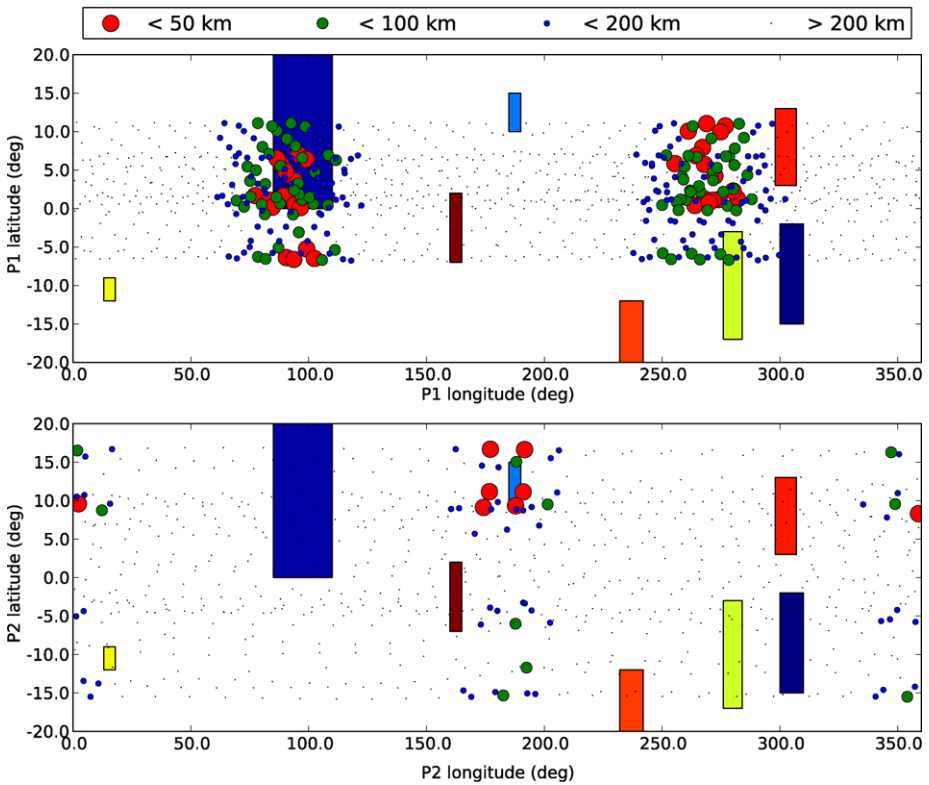


Fig. 15 Periape locations at the Moon during four years of lunar orbits. Periape altitudes are affected by perturbations due to Earth’s gravity so that they are lowest at constrained longitudes for P1 and P2. The lunar orbits have been tuned to give good coverage of certain magnetic anomalies in the lunar crust (shown as shaded rectangles)

5.4.2 Science measurement opportunities

Figure 12 gives current predictions for the periape altitudes that are expected through the end of 2013. One of the most challenging aspects of the transfer to science orbit was maximizing the number of sub-50 km periapes subject to mission and spacecraft constraints. The science orbits that have been successfully achieved are such that the natural dynamics allow for a number of low periape opportunities. The absence of significant secular drift in the periape altitude helps to minimize the maintenance ΔV needed in the coming years to avoid impact. Planetary-science enhancement burns (PEBs) are planned (but not finalized) to maintain the periape altitude as needed and, ultimately, to lower the apoapsis to increase the number of periapes and reduce the altitude oscillation magnitude.

The science orbits were inclined from the lunar equator, and the periapes were, in part, driven to be so low to allow for better measurements of crustal magnetic anomalies. Figure 15 shows the periape altitude and locations for both spacecraft relative to the lunar surface. The colored boxes indicate the location of some known crustal magnetic anomalies. The inclination oscillation and the secular movement of the argument of periape (Scheeres et al. 2001) induced by the Earth’s gravity allow for a range of periape latitudes at all longitudes. Some of these periapes offer the opportunity for optimal crustal anomaly mea-

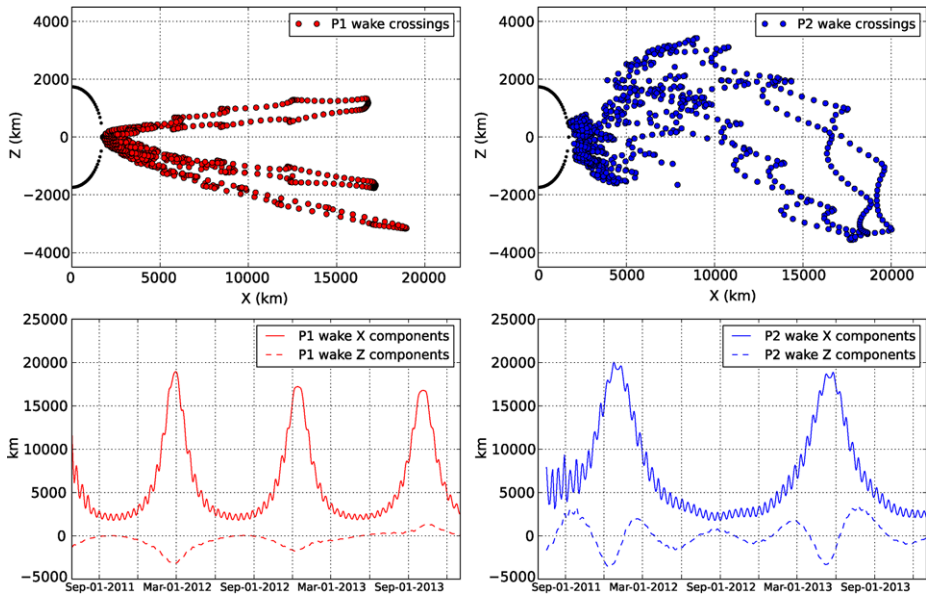


Fig. 16 P1 (red) and P2 (blue) lunar wake observation opportunities during LOI and the lunar orbit phase, with the Moon's limb indicated by *black dots* and the Sun on the $-X$ axis. Each *red* or *blue* point represents an orbit arc within or near the wake. These arcs vary in length and orientation

surements (i.e., sub-50 km altitude near an anomaly). Note that the dynamics dictate that maximum periapsis latitudes are achieved only when inclination is at the minimum of its oscillation cycle.

A key heliophysics objective of the mission is to measure the lunar wake with the two spacecraft in a number of relative geometries over time. Figure 16 shows the range from the Moon's center in the anti-Sun direction of the lunar wake crossing observation opportunities for the achieved ARTEMIS science orbits as a function of time. A large number of measurements opportunities have been created due to the low orbit inclination (one opportunity per orbit per spacecraft), large variety of down-Sun ranges (due to the orbit eccentricity), and relative geometries (due to the orbit precession induced by the Earth).

6 Mission Status

As of February, 2012, both P1 and P2 have successfully arrived into and maintained Lissajous orbits around the Earth-Moon L1 point, transitioned into lunar orbit insertions, and reduced their orbit periods into the science orbit. Both probes and their instruments are functioning normally. One minor surprise occurred on October 14, 2010, when a small, sudden change was observed in the velocity and spin rate of P1, which was quickly traced to the loss of the EFI sensor ball at the end of one of the four EFI booms deployed from the sides of the probe. This loss was originally attributed to a micrometeorite severing the fine wire that connected the sensor ball to the preamp at the end of the boom (http://www.nasa.gov/mis-sion_pages/themis/news/artemis-struck.html), but then the preamp separated from the same boom on August 27, 2011. This suggests that in the earlier event a micrometeorite impacted and weakened the connection between the boom and the

preamp. In this scenario the shock of the impact at the other end of the preamp caused the fine wire to the sensor to break immediately, while thermal cycling and various mechanical strains finally broke the preamp loose later (Owens et al. 2012).

Although reduction in the number of EFI sensors will cause a slight reduction in the quality of the electric field measurements, the instrument still satisfies its science requirements. The loss of the sensor mass also shifted the probe's center of mass, which has and will complicate operations somewhat, especially in the management of the propellant on board, and affect the mission design because side maneuvers now have a much larger (though still small in absolute terms at -0.05 RPM per m/s) effect on the spin rate.

Table 2 shows how the maneuver ΔV s added up for all of the phases.

7 Conclusions

The trajectory design of the ARTEMIS mission that began in July of 2009 has been presented here. The design sent two probes from Earth orbit to the Moon via a transfer that took ~ 2 years and involved numerous lunar approaches and flybys, low-energy trajectory legs in the Earth-Sun system, and Lissajous orbits around the Earth-Moon Lagrange points on either side of the Moon, and finally culminated with both probes in very eccentric low-lunar orbits. The constraints imposed on the design by the limitations of the THEMIS probes (which were designed for an Earth-orbiting mission)—including thruster orientation, available ΔV , maximum shadow capability, maximum distance for radio telecommunication, and thruster capabilities—necessitated an innovative design. Ultimately the design satisfied all mission constraints and offers a variety of scientific measurement opportunities that have the potential to enhance understanding of Earth-Moon-Sun interactions.

Given the challenges that the ARTEMIS mission presented and the complexity of the design needed to meet those challenges, it is notable that the cost of the mission design effort was many times less than one would estimate for a new, i.e., non-extended, full mission of comparable difficulty. One major difference is that ARTEMIS started in space with given orbits for the two probes, saving the significant cost of determining a launch period and optimal launch targets for the mission. But an even bigger factor in cost savings was acceptance of risk that is unacceptable for a more expensive mission. The THEMIS mission was already a success and completely justified the investment already made in building and launching the probes. Furthermore, the outermost two probes were forced to find a new mission because the THEMIS orbits they were in would have led to fatal shadows by now. So in a sense the only thing at risk was the cost of the ARTEMIS design itself, leading to a situation where the investment at risk was reduced by accepting a higher probability that the risk would be realized.

The primary cost-saving characteristic of the mission design process that put ARTEMIS at risk was the near absence of redundancy, both in the design process and in the products of that process. There is a certain amount of natural redundancy in the use of two probes, and indeed much of the opportunity for new science could be realized even in the absence of one. A significant opportunity would have been missed, though, without the dual measurements that have already been made by the two probes and that are planned for the remainder of the mission. On the ground, however, the design team was pared down so that at times it relied on a single person; had that person been unavailable, a different and uncertain approach for that part of the design would have been required. The limited team size also meant that the design itself was nearly "single string" in the absence of backup and contingency trajectories. The analysis that would have produced such alternative designs was most often replaced

by engineering judgment that such alternatives existed and could be found if needed. Similarly, in the area of maneuver design, extensive Monte Carlo runs covering all the ways that reality could diverge from the nominal plan were replaced by experience-based estimates of when trajectory correction maneuvers might be needed and of how much ΔV capability might be needed to correct the trajectories as they were flown.

The greatest uncertainty in the design was perhaps in the area of trans-lunar trajectory corrections because these could contain only minimal ΔV components in the direction of the probe $-Z$ axis. In one of the rare instances of backup analysis, an alternative transfer that included deterministic “down” maneuvers at strategic points along the way was designed; these maneuvers could serve to enable upward corrections by reducing the size of the down maneuvers. But this alternative transfer was not used or needed, and the maneuver design team was able to design TCMs in flight that kept the probes on track to their Lissajous rendezvous. The enabling mitigation of the probe’s thrust-direction constraints was that every phase of the mission, including the transfer phase, included multiple orbits of the Earth or Moon so that an up maneuver on one side of the orbit could be replaced by a down maneuver or in some cases a radial maneuver elsewhere in the orbit. Another critical factor of mission success so far has been the stellar performance of the two probes and the mission operations team: every one of the dozens and dozens of maneuvers has been executed as planned.

Acknowledgements The work described in this paper was carried out in part at the Jet Propulsion Laboratory, California Institute of Technology, under a contract with the National Aeronautics and Space Administration.

The authors would like to recognize and compliment the outstanding contributions of the THEMIS/ARTEMIS science team, the ARTEMIS mission design team at the Jet Propulsion Laboratory, the ARTEMIS navigation and maneuver design team at Goddard Space Flight Center, and the THEMIS/ARTEMIS navigation, maneuver design, and operations team at the University of California-Berkeley Space Science Laboratory to the successful development and implementation (so far) of the ARTEMIS mission. Judy Hohl, our editor at UCLA, and Emmanuel Masongsong, our graphics editor at UCLA, contributed significantly to the readability of this paper. The maneuver data in the tables above were supplied by Dan Cosgrove, the THEMIS/ARTEMIS Navigation Lead.

References

- V. Angelopoulos, The THEMIS Mission. *Space Sci. Rev.* **141**, 5–34 (2008). doi:[10.1007/s11214-008-9336-1](https://doi.org/10.1007/s11214-008-9336-1)
- V. Angelopoulos, The ARTEMIS Mission. *Space Sci. Rev.* (2010). doi:[10.1007/s11214-010-9687-2](https://doi.org/10.1007/s11214-010-9687-2)
- V. Angelopoulos, D.G. Sibeck, THEMIS and ARTEMIS. A proposal submitted for the Senior Review 2008 of the Mission Operations and Data Analysis Program for the Heliophysics Operating Missions. Available at http://www.igpp.ucla.edu/public/THEMIS/SCI/Pubs/Proposals%20and%20Reports/HP_SR_2008_THEMIS_SciTech_20080221.pdf (2008)
- D. Auslander, J. Cermenska, G. Dalton, M. de laPena, C.K.H. Dharan, W. Donokowski, R. Duck, J. Kim, D. Pankow, A. Plauche, M. Rahmani, S. Sulack, T.F. Tan, P. Turin, T. Williams, Instrument boom mechanisms on the THEMIS satellites; magnetometer, radial wire, and axial booms. *Space Sci. Rev.* **141**, 185–211 (2008). doi:[10.1007/s11214-008-9386-4](https://doi.org/10.1007/s11214-008-9386-4)
- J.V. Breakwell, J.V. Brown, The halo family of 3-dimensional periodic orbits in the earth-moon restricted 3-body problem. *Celest. Mech.* **20**, 389–404 (1979)
- S.B. Broschart, M.K. Chung, S.J. Hatch, J.H. Ma, T.H. Sweetser, S.S. Weinstein-Weiss, V. Angelopoulos, Preliminary trajectory design for the Artemis lunar mission, in *AAS/AIAA Astrodynamics Specialists Conference, Pittsburgh, Pennsylvania*, ed. by A.V. Rao, T.A. Lovell, F.K. Chan, L.A. Cangahuala. Advances in the Astronautical Sciences, vol. 134 (Univelt, Inc., San Diego, 2009). American Astronautical Society/American Institute of Aeronautics and Astronautics
- S.B. Broschart, T.H. Sweetser, V. Angelopoulos, D.C. Folta, M.A. Woodard, Artemis lunar orbit insertion and science orbit design through 2013. Presented at the 2011 AAS/AIAA Astrodynamics Specialists Meeting, Girdwood, AK, July 31–August 4, 2011, AAS paper 11-509 (2011)
- M.K. Chung, V. Angelopoulos, S. Weinstein-Weiss, R. Roncoli, N. Murphy, *Personal email communications, August 13–19* (2005)

- R. Farquhar, The utilization of halo orbits in advanced lunar operation. Technical report TN-D6365, NASA, GSFC, Greenbelt, MD, 1971
- R.W. Farquhar, A.A. Kamel, Quasi-periodic orbits about the translunar libration point. *Celest. Mech.* **7**, 458–473 (1973)
- D. Folta, T.A. Pavlak, K.C. Howell, M.A. Woodard, D.W. Woodfork, Stationkeeping of Lissajous trajectories in the Earth-Moon system with applications to ARTEMIS, in *Advances in the Astronautical Sciences*, pp. 193–208 (2010)
- S. Frey, V. Angelopoulos, M. Bester, J. Bonnell, T. Phan, D. Rummel, Orbit design for the THEMIS mission. *Space Sci. Rev.* **141**, 61–89 (2008). doi:[10.1007/s11214-008-9441-1](https://doi.org/10.1007/s11214-008-9441-1)
- G. Gómez, K. Howell, J. Masdemont, C. Simó, Station-keeping strategies for translunar libration point orbits, in *AAS/AIAA Spaceflight Mechanics 1998*, ed. by J. Middour, L. Sackett, L. D'Amario, D. Byrnes. *Advances in the Astronautical Sciences*, vol. 99 (Univelt, Inc., San Diego, 1998), pp. 949–967
- P. Harvey, E. Taylor, R. Sterling, M. Cully, The THEMIS constellation. *Space Sci. Rev.* **141**, 117–152 (2008). doi:[10.1007/s11214-008-9416-2](https://doi.org/10.1007/s11214-008-9416-2)
- D. Hoffman, Stationkeeping at the colinear equilibrium points of the earth-moon system, Technical report JSC-26189, NASA (1993)
- K.C. Howell, T.M. Keeter, Station-keeping strategies for libration point orbits: target point and floquet mode approaches, in *Proceedings of the AAS/AIAA Spaceflight Mechanics Conference 1995*, ed. by R. Proulx, J. Liu, P. Seidelmann, S. Alfano. *Advances in the Astronautical Sciences*, vol. 89 (Univelt, Inc., San Diego, 1995), pp. 1377–1396
- K.C. Howell, B.T. Barden, M.W. Lo, Application of dynamical systems theory to trajectory design for a libration point mission. *J. Astronaut. Sci.* **45**(2), 161–178 (1997)
- W.S. Koon, M.W. Lo, J.E. Marsden, S.D. Ross, Heteroclinic connections between periodic orbits and resonance transitions in celestial mechanics. *Chaos* **10**(2), 427–469 (2000). doi:[10.1063/1.166509](https://doi.org/10.1063/1.166509)
- B.D. Owens, D.P. Cosgrove, J.E. Marchese, J.W. Bonnell, D.H. Pankow, S. Frey, M.G. Bester, Mass ejection anomaly in Lissajous orbit: response and implications for the Artemis mission. Presented at the 2012 AAS/AIAA Spaceflight Mechanics Meeting, Charleston, SC, Jan. 29–Feb. 2, Paper AAS 12-181 (2012)
- C. Renault, D. Scheeres, Statistical analysis of control maneuvers in unstable orbital environments. *J. Guid. Control Dyn.* **26**(5), 758–769 (2003)
- D.J. Scheeres, M.D. Guman, B.F. Villac, Stability analysis of planetary satellite orbiters: applications to the Europa orbiter. *J. Guid. Control Dyn.* **24**(4), 778–787 (2001)
- M. Sholl, M. Leeds, J. Holbrook, THEMIS reaction control system—from I&T through early orbit operations, in *Proceedings of the 43rd AIAA/ASME/SAE/ASEE Joint Propulsion Conference & Exhibit*, Cincinnati, OH, USA, 8–11 July 2007 (2007)
- G.J. Whiffen, *Static/dynamic for optimizing a useful objective*, United states patent, No. 6,496,741. Issued December 2002 (1999)
- G.J. Whiffen, Mystic: implementation of the static dynamic optimal control algorithm for high-fidelity, low-thrust trajectory design, in *Proceedings of the AIAA/ASS Astrodynamics Specialists Conference*, Keystone, Colorado (2006) Paper AIAA 2006-6741
- M. Woodard, D. Folta, D. Woodfork, 2009 ARTEMIS: the first mission to the lunar libration points. Presented at the 21st International Symposium on Space Flight Dynamics, Toulouse, France